Dynamic analysis of periodic structures

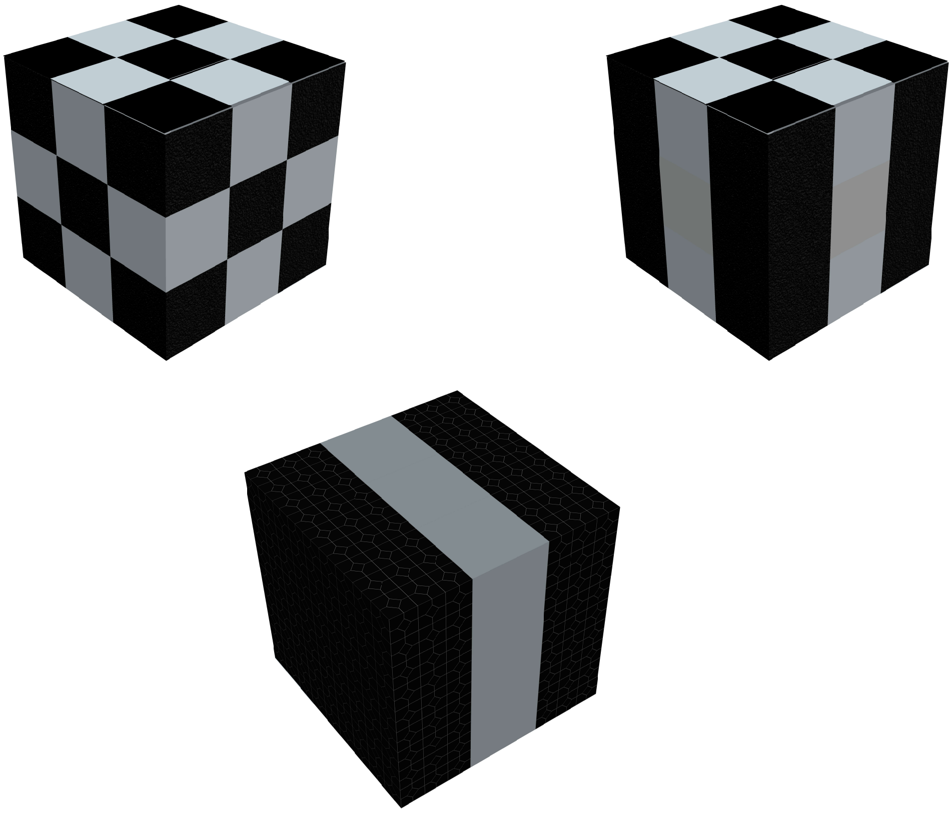

Master Thesis
Samsor Sohil
School of Engineering and Science
Aalborg University

9. January 2017

AALBORG UNIVERSITY
STUDENT REPORT

School of Engineering and Science
Thomas Manns Vej 23
9220 Aalborg Ø
Telephone 99 40 85 30
www.civil.aau.dk

Title:

Dynamic analysis of periodic structures

Project:

Master Thesis in Structural and Civil Engineering

Project period:

September 2016 - January 2016

Student

Samsor Sohil

Supervisor:

Lars V. Andersen

Printed editions: 3
Number of pages: 75
Appendix: External CD
Finished 09-01-2017

Synopsis:

The following report contains the dynamic analysis of a periodic structure. The project has three main parts. The first part explains the basic mathematics behind vibration followed by the studies done in the field of periodicity in structural and civil engineering.
The second part deals with the finite element analysis in structural dynamics. The basics of finite elements theory is explained here. The chapter starts with a simple beam problem in order to build a smooth transition to the dynamic analysis of periodic structures with the main focus on Floquet's theory. First free-free and fixed-fixed boundary conditions are applied to the beam, thereafter a one-dimensional waveguide is analysed.
As the idea of periodicity and dynamic analysis of a one-dimensional waveguide is clarified, chapter three deals with implementation of periodicity in two-dimensions in a unit cell, where again the analysis is based on Floquet's theory. The dispersion curves for all the aforementioned periodic cells are plotted and compared.

Preface and reading guide

This report is written by Samsor Sohil student at 4th semester of the Master's Program in Structural and Civil Engineering under the School of Civil Engineering and Science at Aalborg University. The main topic is Dynamic Analysis of Periodic Structures. The project contains 4 chapters, where each chapter contains sections and subsection. For illustration of references Harvard Method is used, where last name appears first followed by the years. As for the bibliography, books referred to by author and title. Articles specified by the name first followed by the year and the information available on each article.

The number for the figures and tables are based the chapters location, for example 2.5 refers to the fifth figure in chapter two. The caption for the tables are place above the tables, while for figures it is placed beneath the figures.

The project is submitted on ninth of January 2017. More greatly goes a special thanks to committed and resourceful supervisor of this project associate professor Lars Vabbersgaard Andersen for his devoted guidance and help towards a successful completion of this work.

Samsor Sohil

Contents

1 Introduction

In the field of structural and civil engineering, vibration is a major challenge. Vibration can be undesirable and depending on its magnitude it can be very harmful. The source of vibration for example from an elevator, a railway track as in Figure 1.1 or machinery etc. can be really disturbing in the populated areas, natural born vibration can be even worse. Natural born vibrations such as earthquakes are seen to cause major destruction which leads to both human and economic loss. Hence it is very necessary to prevent the vibration either by eliminating its source or by reducing it as much as possible, so it does not cause harm to people and environment. In Figure 1.1 three examples of vibration sources are illustrated, which people faces every day.

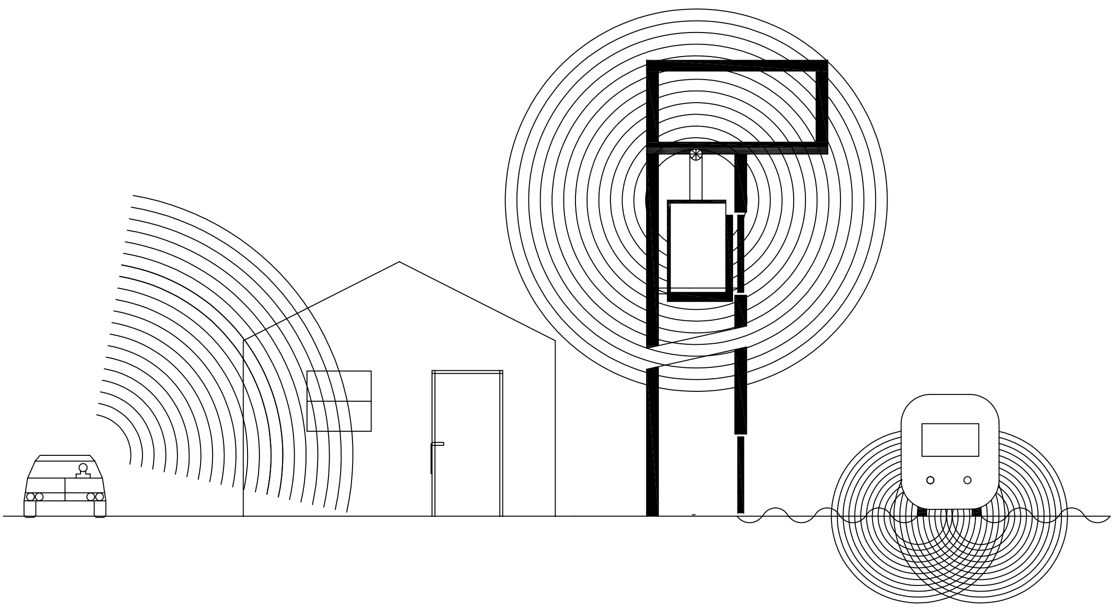

Figure 1.1. Human-made vibration source.

Reducing this vibration can be done in several ways such as applying isolation, damping devices, implementing a periodically (repeated) geometry or even fully eliminating the source of vibration. All of these solutions can solve most of these problems, but some of these solutions mentioned are either physically of economically impossible, for example eliminating the source of earthquake is an impossible job. Therefore a solution is needed to face this problem and reduce its effect as much as possible, so at the end the loss of humans and environment is as minimal as possible. Not only earthquakes but also the unnecessary noise and vibration from traffic, train tracks, machinery and so on, shall be minimized as much as possible so it does not disturb the population or in worst case force people to leave for a quite place.

In this rapport a solution will be presented, which is thought to be effective in attenuation of vibration. The economical side of this solution is not covered in this project. The solution is based on implementing periodic structure for attenuation of vibration. Some of the examples for a periodic structures can be illustrated in the following Figures.

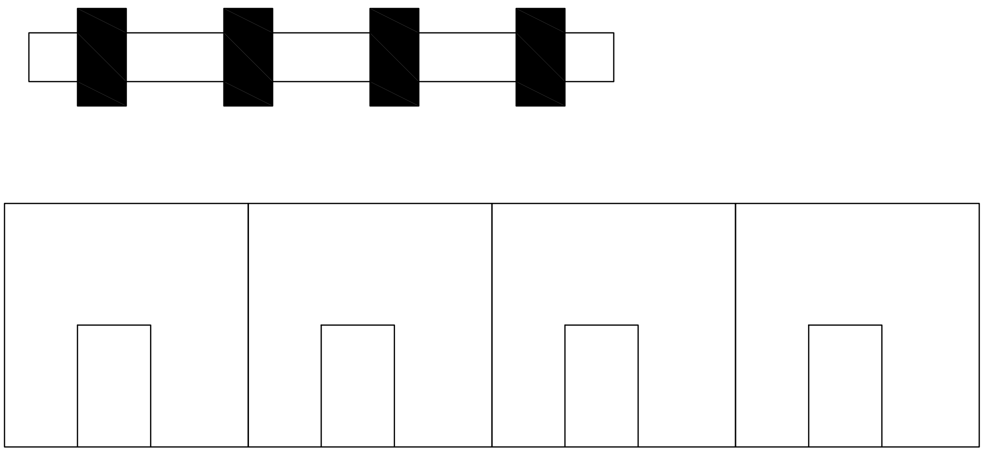

Figure 1.2. The picture on top shows a cylinder with repeated bands, which makes a periodic structure. The picture below show a wall panel in a repeated manner i.e a periodic wall.

The Figure above in 1.2 illustrates some of the typical periodic structures are illustrated. The purpose of the this project is to show that periodic structures work as a filter. The project is limited to periodicity in only two dimensions. [1]

[1] periodic figure måske en fra manconi

This project is made of three parts. The first part starts with an introduction to vibration and the challenges vibration presents in the field of structural and civil engineering followed by its effect on people's lives. The chapter moves on by presenting the basic theory of wave propagation in material and how it behaves as it meets an obstacle. Here reflection and transmission of waves are shortly explained. Furthermore expressions like dispersion and dissipation are explained and clarified. The first part finishes with presentation of periodicity in the field of structural and civil engineering through a number of articles. In this regard works of some of the scientists are shortly presented and described for what they have done in this area.

The second part of the project starts with finite elements in structural dynamics. Here the basic theory of finite elements in dynamics is presented, where the main focus is on bar and beam elements. Both stiffness- and mass matrices for bar and beam elements together with equation of motion are described.

This chapter's main focus is on study of natural frequencies and modes, where it starts with a simple problem by extracting the eigenfrequencies of a beam in finite element programs Matlab and COMSOL multiphysics. The results from these two programmes are then compared with each other. Different models like "beam" and "solid" models are tested in COMSOL and compared among each other and MatLab. Through the chapter two types of boundary conditions free-free and fixed-fixed, are used. This part is finished with a short discussion of the results

The third part of the project deals with dynamic analysis of periodic structures. The chapter starts by explaining Floquet's theory and dynamics of a periodic unit cell. In this relation finite elements theory of a one-dimensional waveguide is presented. Build on this theory a one-dimensional waveguide is analysed with Free-free, fixed-fixed and periodic boundary conditions in both COMSOL and MatLab, hereafter the modes are compared from both programmes. This is done to make sure both programmes delivers the same results and the results deliver by COMSOL are reliable before moving on. After giving a satisfactory result a complex geometry was only build in COMSOL as in this stage no approval was needed from finite element programme MatLab as COMSOL was tested through the whole project and the results were trusted. In this section not only the the geometry of the cell was optimized but also two-dimension periodic boundary conditions are given to the cell instead of one-dimension. Additionally dispersion curves from a unit cell with periodicity in one-dimension are compared with a unit cell having periodicity in two-dimension.

The project is finished with a conclusion and discussion of the results.

Vibration 2

In the subsequent section an explanation of how the waves propagate in elastic and viscoelastic material will be presented.

2.1 Wave propagation in elastic and viscoelastic media

A well-known source of waves in elastic soil media is earthquakes. Earthquakes are not the only source of waves. Man-made ground vibration such as sheet piling, traffic induced vibration, noise from machine foundation has a major impact on people and buildings, therefore many authors have studied the impact of this vibration.

Unlike steel and other metals which may be considered as homogeneous even on a microscopic level, concrete, rocks and soil are considered inhomogeneous as their particles vary in sizes and shapes. Not only sizes and shapes of particles vary but the local density of materials varies too, due to the void ratio. However this aspect plays no major role in wave propagation. The local inhomogeneities mean that the characteristic wavelength is way bigger than the variation of material properties over a distance. Thus only inhomogeneities such as layers of different soil deposits (strata) are important for low frequencies, whereas in high frequencies or for coarsely grained materials, wave propagation can be affected by the size and shape of the grains.

This local and global inhomogeneities also apply to the dynamics of structures, for example low frequencies and vibration modes are weakly affected by features as welding, joints and bolts, while features as variations of the bending stiffness of beams strongly affects the response.

A material being isotropic or anisotropic also has a big influence on the speed of wave propagation, as in isotropic material the speed of the wave propagation is the same in all directions, however in anisotropic material the wave speed differs from one direction to another. In elastic media there are primarily two types of waves that propagates, dilatational waves and rotational waves.

2.1.1 Dilatational waves

In this particular case the motion of particle is pure dilatation or pressure, with the phase velocity c_P Figure 2.1. These type of waves are explained by the following Navier's equation in the absence of body force.

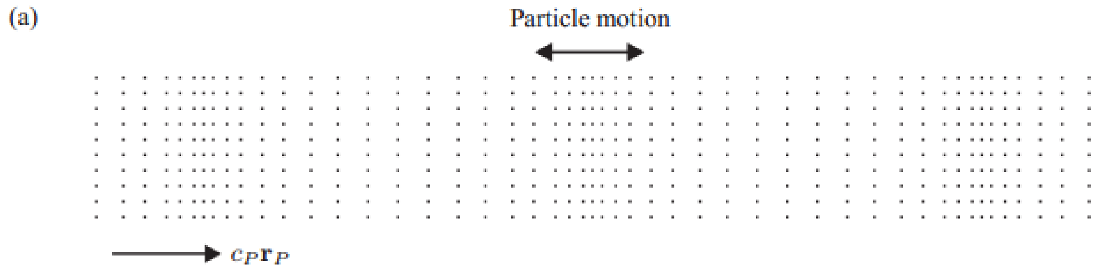

Figure 2.1. The particle motion in P-waves. The unit vectors r_P denote the directions of P-wave propagation. [Andersen, 2006].

$$\frac{\partial^2 \Delta}{\partial x_i \partial dx_i} = \frac{1}{c_P^2}\frac{\partial^2 \Delta}{\partial t^2} \qquad \textit{where} \qquad c_P = \sqrt{\frac{\lambda + 2\mu}{\rho}} \tag{2.1}$$

The above equation 2.1 is valid for three dimensional wave propagation where the constants in phase speed c_P are the so-called Lamé constants shown below:

$$\lambda = \frac{\nu E}{(1+\nu)(1-2\nu)} \qquad \nu = \frac{\lambda}{2(\lambda + \mu})$$

Alternatively it can be written as follow

$$E = \frac{\mu(3\lambda + 2\mu)}{\lambda + \mu)}, \qquad \nu = \frac{\lambda}{2(\lambda + \mu)}$$

And $\Delta = \Delta(x, t)$ illustrates the dilation.

2.1.2 Rotational waves

Contrary to dilatational waves, the motion of the particle is equivoluminal shear as in Figure 2.2, The speed of rotational waves is less than dilatational waves, where the phase velocity c_S is around $0.5c_P$ and lower depending on Poisson's ratio. With the phase speed c_S the three-dimensional wave equation is described as follow.

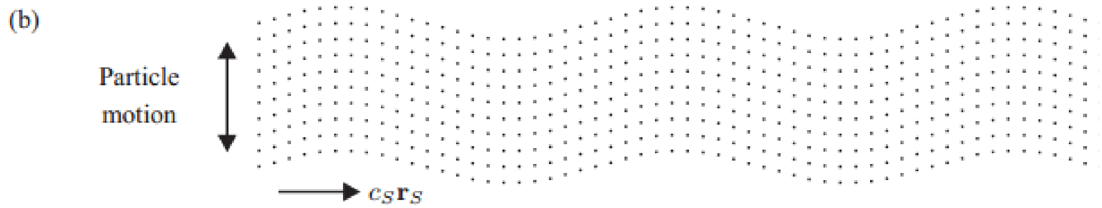

Figure 2.2. The particle motion in S-waves. The unit vectors r_S denote the directions of S-wave propagation. [Andersen, 2006]

$$\frac{\partial^2 w_i}{\partial x_j \partial x_j} = \frac{1}{c_S^2}\frac{\partial^2 w_i}{\partial t^2} \tag{2.2}$$

Where w_j is the rotation of the displacement field and the phase velocity is shown as:

$$c_S = \sqrt{\frac{\mu}{\rho}}$$

The question remains what if the waves meet a barrier or an obstacle on its path. This question will be answered in the next section.

2.2 Reflection and transmission of waves

2.2.1 Reflection at free or fixed boundary

When a wave hits a barrier or an obstacle, it will be reflected either fully or partially. This reflection is mainly dependent of the boundary conditions. This phenomenon is demonstrated in details through an example in [Andersen, 2006]. In case of one-dimensional wave propagation where mass density is ρ and wave velocity is c the displacement field governed by (2.1) and (2.2) for one-dimensional wave propagation in the presence of body force $b = b(x,t)$ is as follow.

$$\frac{\partial^2 u}{\partial x^2} + \frac{\rho b}{c^2} = \frac{1}{c^2}\frac{\partial^2 u}{\partial t^2} \tag{2.3}$$

Note that the body forces are applied per unit length in x-direction, as the material domain covers the distance of $x \geq 0$ and the boundary is located at $x = 0$. As the waves hit the boundary, reflection will occur. Now the wave field contains both incident waves propagating in positive x-direction and reflected waves propagating in the opposite direction as in Figure 2.3. Hereby the displacement field can be written as follows, assuming no change will happen in waves shape or amplitude.

$$u(x,t) = U^i f(ct + x) + U^r f(ct - x) \tag{2.4}$$

Where U is the constant amplitude and the index i and r refer to incoming and reflected and f is a function describing the shape and propagation of waves. Equation (2.4) is considered a valid solution to the wave equation (2.3).

The boundary the wave hits can can be either moveable of fixed. These two different types of boundaries are:

- Dirichlet conditions or natural boundary conditions as $u(0,t) = 0$
- Neumann conditions or mechanical boundary conditions as $-\partial u/\partial x = 0$

Dirichlet conditions corresponds to a fixed boundary, i.e. an unmovable boundary for example soil over bedrock. Using the solution in (2.4) the boundary condition gives:

$$u(0,t) = U^i f(ct) + U^r f(ct) = 0 \tag{2.5}$$

Where the following has to be fulfilled for any instance of time t.

$$U^i + U^r = 0 \qquad\qquad U^r = C_r U^i \tag{2.6}$$

Where the reflection coefficient is $C_r = -1$. In this type of boundary conditions there will be a phase shift of π between the incident and the reflected wave shown by the change in sign. This type of waves is depicted in Figure 2.3 on the left.

However in the second condition (Neumann condition) the boundary is free, and both reflected waves and incident waves are in phase as in Figure 2.3 on the right.

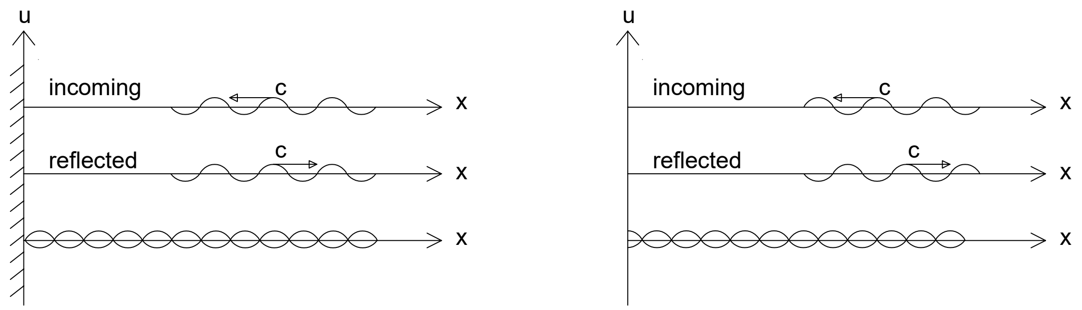

Figure 2.3. Fixed boundary on the left and moving boundary on the right.

Applying this boundary condition the following is obtained

$$\left.\frac{\partial u}{\partial x}\right|_{x=0} = U^i f'(ct+x)\big|_{x=0} - U^r f'(ct-x)\big|_{x=0} = 0 \tag{2.7}$$

And the same relation as above shall be fulfilled if equation (2.3) has to be applicable for arbitrary t as in follow.

$$U^i - U^r = 0 \qquad \Rightarrow \qquad U^r = C_r U^i \tag{2.8}$$

As a result it is shown that a full reflection happens in the opposite direction of incident waves. The reflection coefficient here has the value of $C_r = 1$.

As it is illustrated the only difference lies in the phase shifts for the boundaries, other than that the amplitudes for the both cases are equal in both situations and lastly in both cases the incident wave was fully reflected.

2.2.2 Mechanical impedance and transmission coefficient

In case of one-dimensional problem, the mechanical impedance is given as follow

$$z = \rho c \tag{2.9}$$

Where ρ is the mass density of a given material and c is the phase velocity of waves as it propagates through the material. This quantity is included in the following equation (2.10)

$$p(t) = zv(t) \qquad where \qquad v(t) = \dot{u}(0,t) \tag{2.10}$$

Here $v(t)$ is defining the particle velocity at the boundary and $p(t)$ is defining the traction. Equation (2.9) is an important part in the dynamic analysis of material. If a unit traction is applied to a surface, mechanical impedance will provide the particle velocity of the material due to this traction. If c is the phase velocity of sound through the material then the given impedance is called acoustic impedance.

In case of a three-dimensional elastodynamics, where both P- and S-waves are involved, mechanical impedance became a second order tensor z_{ij} and equation (2.10) can be rewritten as follows.

$$p_i(x,t) = z_{ij} v_j(x,t), \qquad x \in S. \tag{2.11}$$

Considering an interface between two materials, the energy transmitted from one material to another is related to their impedance mismatch. This phenomenon will be explained for a one-dimensional case in the following. For a two homogeneous half-spaces with common interface at $x = 0$ where the first half-space is defined by $x \leq 0$ has material with the impedance of $z_1 = \rho_1 c_1$ and the second half-space which is defined by $x > 0$ has the material with the impedance of $z_2 = \rho c_2$.

As the wave hits the interface from the first half-space $x \leq 0$, some of the incoming energy will be transmitted into the second half-space $x > 0$ and the rest of the energy will be reflected back into the first half-space $x \leq 0$ as in Figure 2.4.

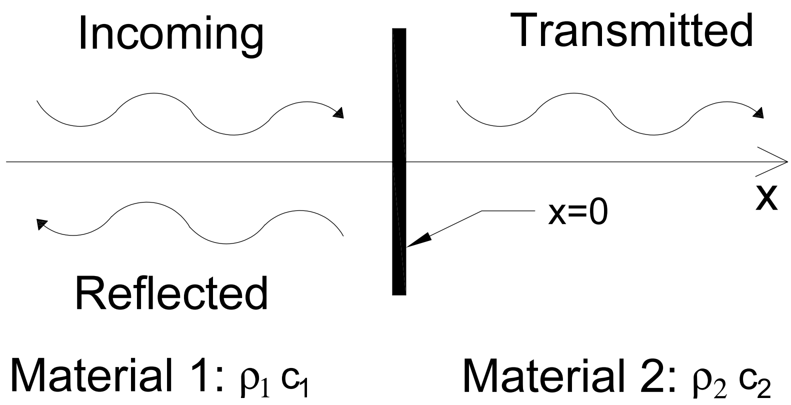

Figure 2.4. Reflection of an incoming SV-wave at a free boundary, where $\theta_P > \theta_S$

As the incoming and reflected waves both propagate in the same material with the impedance of $z_1 = \rho_1 c_1$ and the transmitted waves propagate in a material with different impedance, the following can be stated.

$$z_1 v^i(r) - z_1 v^r(t) = z_2\big(v^i(t) + v^r(t)\big) \Rightarrow \tag{2.12}$$
$$C_r = \frac{v^r(t)}{v^i(t)} = \frac{2z_1}{z_2 + z_2} = \frac{2}{z + \varrho}, \qquad \varrho = \frac{z_2}{z_1}$$

$$z_1 v^i(t) - z_1\big(v^t(t) - v^i(t)\big) = z_2 v^t(t) \Rightarrow \tag{2.13}$$
$$C_t = \frac{v^t(t)}{v^i(t)} = \frac{2z_1}{z_2 + z_2} = \frac{2}{z + \varrho}, \qquad \varrho = \frac{z_2}{z_1}$$

Where

C_r	Reflection coefficient
C_t	Transmission coefficient
$\varrho = \frac{z_2}{z_1}$	Impedance mismatch
$v(t)$	Particle velocity

The relations between these parameters are better illustrated in Figure 2.5. It is clear that the transmission and reflection coefficients only depend on the relative value of the impedances ϱ. If the power per unit area of the surface is equal to zero, i.e. $p(t)v(t) = 0$, then there should be a balance between the power generated by the incoming wave and the power consumed by the reflected and transmitted wave as follow

$$1 = E_r + E_t \quad E_r = C_r^2 = 1 - E_t, \quad E_t = \frac{z_2}{z_1} C_t^2 = \frac{4 z_1 z_2}{(z_1 + z_2)^2} = \frac{4\varrho}{(1+\varrho)^2}, \varrho = \frac{z_2}{z_1} \tag{2.14}$$

Where

E_r	Eneregy-reflection coefficient
E_t	Eneregy-transmission coefficient

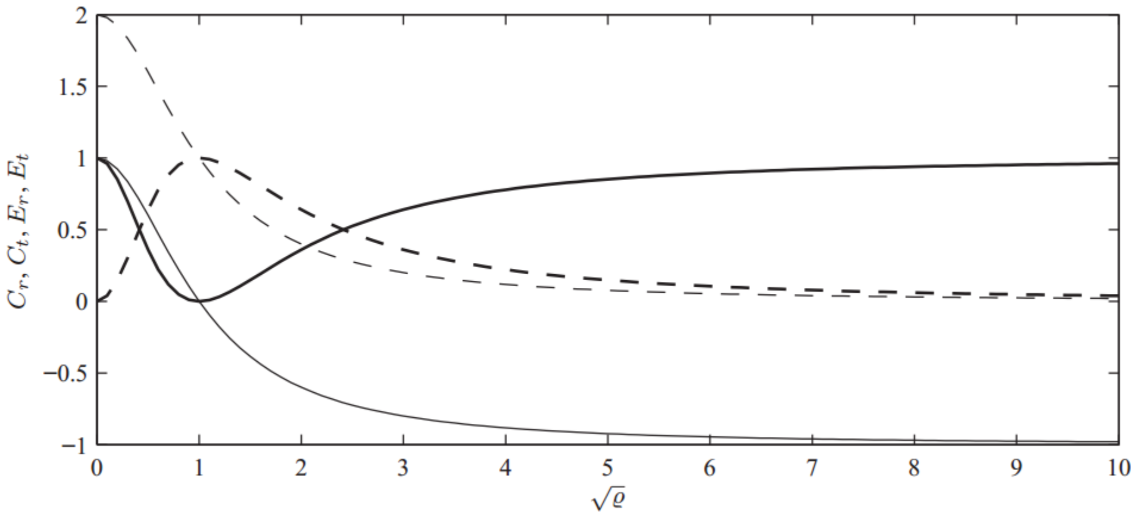

Figure 2.5. Velocity-reflection coefficient C_r(———), velocity-transmission coefficient C_t(- -), energy-reflection coefficient E_r(**———**) and energy-transmission coefficient E_t (**- -**) as a function of the impedance mismatch ϱ [Andersen, 2006]

As it comes from Figure 2.5, when $\varrho = 1$, the corresponding $E_t = 1$, which shows a full transmission of energy. For $\varrho \longrightarrow 0$ the energy-transmission coefficient also goes toward zero $E_t \longrightarrow 0$ which corresponds to a free boundary. And lastly When $\varrho \longrightarrow \infty$, the situation corresponds to a full reflection, where $E_t \longrightarrow \infty$. This shows the behaviour of a fixed boundary.

2.3 Dispersion and dissipation of elastic waves

Another important subject regarded propagation elastic wave is dispersion and dissipation. These two terms describe two different characteristics when it comes to displacement field.

When waves disperse it means, for different wavenumbers waves propagate with different phase speeds, i.e. when the phase speed is dependent on the wavenumber the waves are dispersive, vice versa if waves do not depend on wavenumbers the waves are non-dispersive.

Dissipation on the other hand is wave attenuation or damping over time and/or space as seen in Figure 2.6 . This damping can be from both geometrical dissipation and material dissipation [Andersen, 2006].

2.3.1 Eigenvalues and there relation to dissipation of waves.

According to Table 2.1 eigenvalues $|\lambda_i| < 1$ shows the waves travelling in the positive direction and the set of eigenvalues with $|\lambda_i| > 1$ travels in the negative direction.

The waves shown above in Figure 2.6 can be associated with wavenumbers in Table 2.1. The eigenvalues are generally in complex form, the following can be written.

$$\lambda = e^{-\mu\Delta}e^{ik\Delta} \tag{2.15}$$

Where μ is the change in amplitude, k is the change in phase $i = \sqrt{-1}$. Assuming no damping in the system, the amplitude of propagating waves will remain constant, with $|\lambda_j| = 1$, $\mu_j = 0$ and $\lambda_j = e^{-k\Delta}$ since

$$|e^{ix}| = 1 \qquad forall \qquad x \in \mathbb{R}$$

The relation between the eigenvalues and the above-mentioned waves can be described in the following Table 2.1

Table 2.1. Properties of eigenvalues and associated waves

λ	$\|\lambda\|$	μ	k	wave	direction
imaginary	1	0	> 0	propagating	
real	< 1	> 0	0	evanescent	positive
complex	< 1	> 0	> 0	attenuating	
imaginary	1	0	< 0	propagating	
real	> 1	< 0	0	evanescent	negative
complex	> 1	< 0	< 0	attenuating	

Lastly evanescent waves given by $|\lambda_j| \lesseqgtr 1$ are characteristic for decaying exponentially with distance i.e. the amplitude decreases in the direction of wave propagation. This decrease happens with a factor of $e^{-\mu\Delta}$ over the length Δ. They are known to be localized and not able to carry energy. It shall be mentioned that this decay happens without oscillation. On the other hand an attenuating wave oscillates with the wavenumber k meanwhile the amplitude decays by $e^{-\mu\Delta}$. The different types of waves are illustrated in the following [L.Hinke and Brennan, 2004].

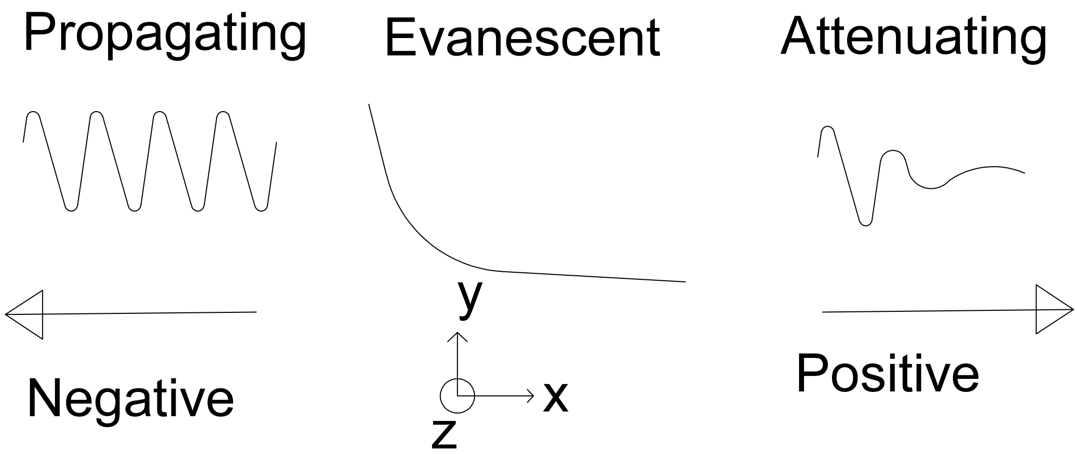

Figure 2.6. Different type of waves.

The topic of wave propagation is clarified, it is also illustrated how waves are reflected. In the following periodicity in structural and civil engineering will be presented through a number of articles and researches done by some scientists. It will be explained how periodic structures are used in this particular field and how a periodic structure affects the propagation of vibration.

2.4 Periodicity in structural and civil engineering

As mentioned in the beginning of the chapter, vibration is a major challenge in the field of structural and civil engineering. A solution proposed in this rapport is the so-called *periodicity*. Periodicity is a very broad subject in the field of structural civil engineering. Periodicity is not only introduced in the field of engineering but also in physics, natural sciences, economics, and finance. In the previous section propagation of wave in material is explained. However this propagation is strongly dependent on the formation of a structure in which the waves are propagating within. If the waves do not face any obstacle on their path then the attenuation will be very weak, but if there are obstacles in their path, then the waves will attenuate quickly, as these obstacles will act like a filter for example in a periodic structure. This claim will be supported in the following chapter.

A periodic structure can be defined as a structure consisting of substructures with identical geometry, coupled together in a regular manner. Periodicity can have different forms based on the arrangements, fx linear in line bridges or multi-storey buildings, axisymmetric in shells or even two or three dimension as in framed roofs.

Using the periodic property of the aforementioned structures can lead to greater simplification of dynamic analysis [A.Y.-T.Leung, 1980]. In the following Figure 2.7 a simple concept of one-,two- and three-dimension periodicity is illustrated.

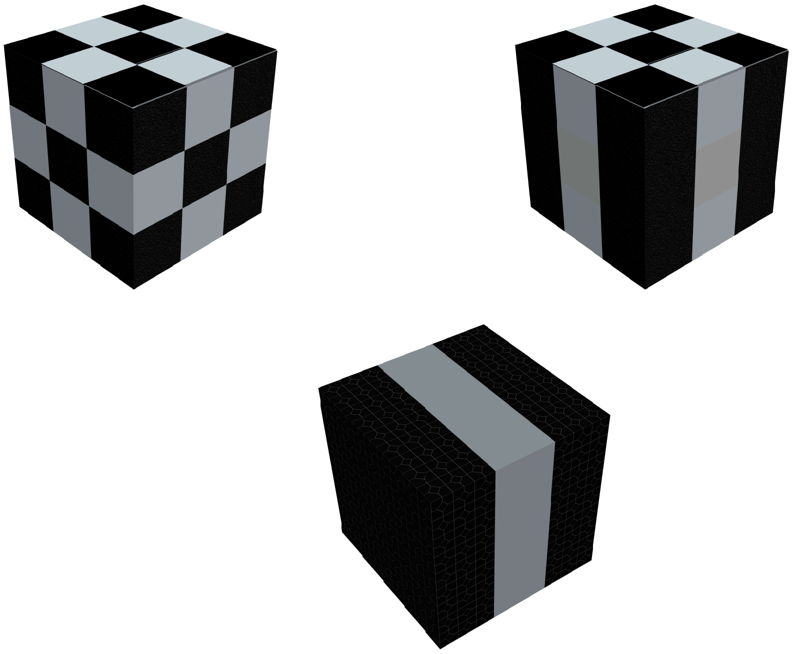

Figure 2.7. Periodic structures. Three-dimension periodic structure upper left, two-dimension periodic structure upper right and one-dimensional periodic structure under.

The idea of adding periodicity to structures is to reduce and mitigate vibrations and noise transmission. By implementing periodicity, the vibration from these sources can be significantly reduced. Periodic structures act as a filter, which exhibits stop band or band gaps where propagation of waves is not possible and thereby no energy flow takes place. In case where the waves are propagated, energy will be transmitted i.e. pass bands are exhibitet [Andersen, 2015].

Recently these so-called band gaps are also mentioned in [Domadiya and Andersen, 2014]. The paper presents the numerical investigation of stop-band in one-dimension periodic structure. A similar example is done in chapter three. This study was also accompanied with an experimental investigation. The paper points out that, the periodic nature of the structure is the reason at which stop-bands occur at some particular frequencies and this periodicity can be used as a filter for attenuation of vibration. Propagation of waves through these stop-bands is impossible and the only way the waves can propagate will be through pass-bands. The article presents implementation of Floquet's theory in periodic one-dimension waveguides followed by numerical examples and experimental validation. For more on Floquet's theory refer to chapter three. The results show that the natural frequencies extracted from the experimental frequency-response approve the simple supported boundary conditions. The article concludes that only a few number of cells are sufficient for the reduction of noise.

[Huang and Shi, 2013] use the periodic pile barriers as in Figure 2.8 to create band of frequency gaps in order to reduce the dynamic response of the structures. The paper investigated the benefit of designing the pile barriers based on periodic theory for reducing the horizontal vibration.

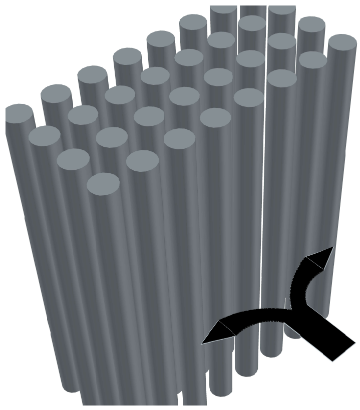

Figure 2.8. Barrier pile arranged in periodic manner.

Accordingly [Gaofeng and Zhifei, 2010] created frequency gap using periodic foundation. The idea of creating periodic foundation was to illustrate, that periodic structures can also be effective in attenuation of seismic waves, which was shown to be true. [H J Xiang and Mo, 2012] did an experimental validation of vibration attenuation in layered foundation. The experiment consisted of scaled model frame, periodic foundation and a shake table. Together with the analytical results a shake table test was done on the periodic foundation. Their results showed that, as the exciting frequencies fell into the band gaps a strong vibration mitigation appears. It was also highlighted that the periodic foundation has also the capability to isolate not only the horizontal vibration but also the vertical vibration. Their tests showed that periodic foundations can work as a multi-dimensional base isolation, but they are less effective when it comes to mitigation of vibration when exciting frequency was found outside of the band-gaps.

Numerous authors through numerical and experimental investigation have studied the concept of periodicity. Among these authors [Andersen, 2015] has recently studied two cases of periodicity in a stratified ground with two soil layers of different properties, where the first case is the ground with periodic stiffening or ground improvement and the second case the earth surface has a periodic changes in form of artificial landscaping. Again appearance of stop bands and pass bands are illustrated and explained in the article and it is explained how they work in that particular case. In both cases Floquet analysis is used. The paper shows that while barriers or the so-called wave impeding blocks (WIB) are considered as a poor solution in the low frequencies, building periodic changes in the properties of soil demonstrated better results and can be a good alternative compare to the WIB in this particular case.

A similar study is done by [Andersen and Nielsen, 2005], where again the focus is on ground borne noise caused by the movement of load on an embankment Once again the open trenches are preferred compared to the infilled trenches or WIB. A combination of finite elements for modelling track structure, the concrete part of the structure and boundary elements for modelling the subsoil and the infilled trenches are used. Both horizontal and vertical excitation were studied, where both had exhibited different amplifications of response for trench and barriers especially in low frequency as 10 Hz.

Another type of WIB the so-called honeycomb, which surrounds the soil-pile foundation-bridge[1] WIB as Figure 2.9. The two shapes of honeycombs are studied by [Takemiya and Shimabuku, 2002], which are also used to mitigate vibration.

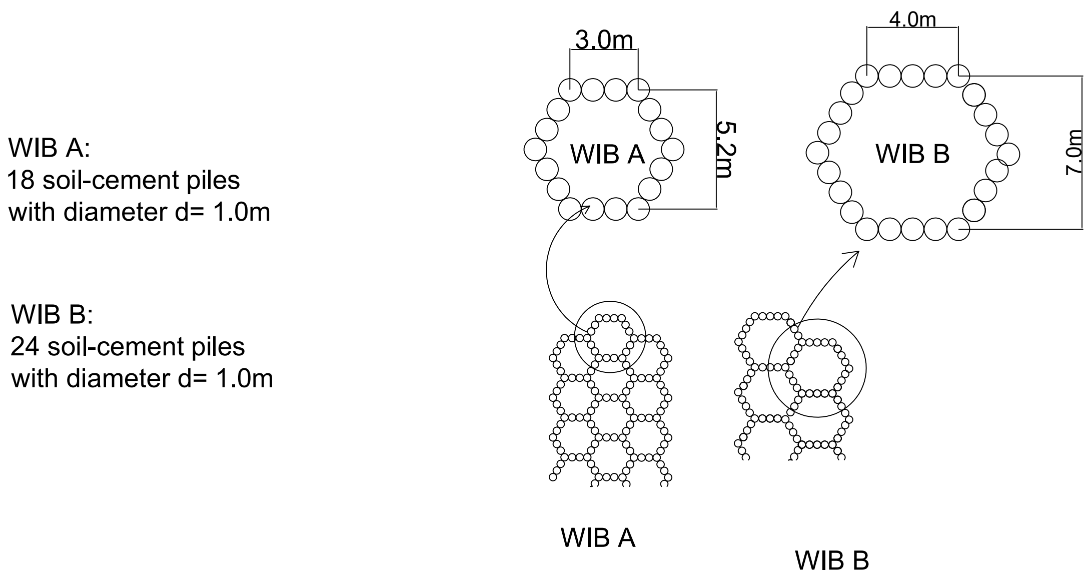

Figure 2.9. WIB A with 24 soil-cement piles, WIB B with 18 soil-cement piles.

[1]The procedure in this particular case is based on mixing cement into the soft ground

Earthquake motion and traffic-induced vibration were the main two types of vibrations which both FEM and BEM used in its analysis. The paper has dealt with seismic and paraseismic problems of a highway bridge at soft site, where the focus was on the soil-improvement-pile foundation system and the reduction of ground vibration by honeycombs. In case of seismic problem ground improvement exhibited better results whereas dealing with traffic-induced vibration honeycomb WIB has presented good results, though the length of horizontal WIB shall be long enough to avoid possible amplifications.

[Jeong and Ruzzene, 2004] studied the behaviour of band-gaps in a two-dimension periodic lattices. One of the main characteristic is the directional behaviour of two-dimensional periodic lattice. In their study they have optimized the geometry of the rectangular lattices in order to maximize the wave attenuation as much as possible. Special attention is given to subjects as Brioullin zones explained in section 4.2.1, Bloch's theorem and phase constant. The structure in question is made of beam elements with circular cross-section rigidly connected with each other which makes a frame-type structure. Their study was concluded by showing the attenuation capabilities of the above-mentioned structure.

In their next study [Jeong and Ruzzene, 2005] did an experimental analysis of the aformentioned two-dimensional grid-like structure, in order to validate the numerical models and design tools done in [Jeong and Ruzzene, 2004]. The unit cell is made of aluminium plate which is suspended by two strings so it acts like a free free boundary conditions. The lattice is excited at one corner and the response is measured in the opposite corner. The exact same condition is provided for the experimental analysis as in analytical, i.e. the lattice is harmonically excited at the same frequency band as in analytical in order to find out whether the observation from both parties are in agreement. The results showed that there was a quantitative and qualitative agreement between the theoretical and experimental results.

From [Jeong and Ruzzene, 2004] and [Jeong and Ruzzene, 2005], it is concluded that the unique directional behavior supports the stop band and pass band patterns. This makes the application of the two dimension periodic structure as directional mechanical filters really attractive. Furthermore these two studies can be supported by another work done by [M.Ruzzene and Scarpa, 2003]. In this work [M.Ruzzene and Scarpa, 2003] have concentrated on a general finite elements technique to model wave propagation in a cellular periodic structures, where mass and stiffness matrices of a single unit cell is utilized. Again Bloch's theorem is used in their study. The study is based on a beam with periodic supports as in, [Mead, 1969], where a periodically supported infinite beam is analysed for free wave propagation. These periodic supports cause the wave to reflect at each support and the so-called "nearfield"[2] effect takes place, therefore in absence of damping a simple sinusoidal wave cannot propagate in such beams. Different types of supports are worked upon in the article especially The term "propagation constant" and its importance is emphasized on.

The way cells are connected with each other can also affect the way waves are propagated from one cell to the next cell, depending on whether the cells are mono-coupled or multi-coupled.

Among others this relation can be studied through two of D.J. Mead's articles. Mead is one of the pioneers who has written many articles about periodic structures. Two of his works [Mead, 1974a] and [Mead, 1974b] relatively mono-coupled and multi-coupled systems, generally describe wave propagation and its relation to natural modes in periodic systems

In [Mead, 1974a] natural frequencies are studied more generally. It is stated that natural frequencies can occur both inside and outside of the propagation zone[3]. Furthermore a different approach is presented on how to determine the natural frequencies. More generally both symmetric[4] and unsymmetrical periodic elements are considered. The article concludes that the bounding frequencies of a periodic system with symmetric elements and the frequencies of the natural modes of a single element which has fixed or free ends are the same and in case of unsymmetrical elements, the natural frequencies will be exhibited inside attenuation zones.

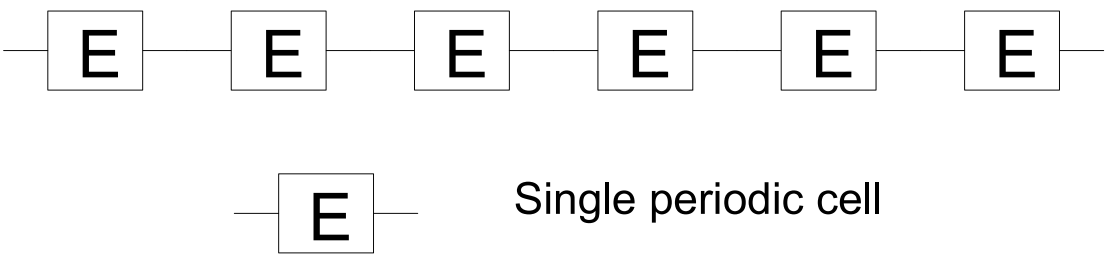

Figure 2.10. Mono-coupled one-dimensional periodic structure.

[Mead, 1974b] is somewhat a developed version of [Mead, 1974a], where instead of a mono-coupled system, harmonic wave propagation in a multi-coupled system is

[2] Previously mentioned as evanescent waves

[3] Propagation zones or previously called pass bands are those distinct frequency bands where energy can be transferred.

[4] A symmetric element has symmetry of mass and stiffness about the mid-point between its ends, whereas an unsymmetrical element does not have this quality. The advantage of symmetry is no change will happen to the the characteristics of the system while reversing the whole system.

analysed. Concepts which are developed in [Mead, 1974a] are used in [Mead, 1974b]. Damping is first introduced in the last part of the article. Although the article concentrates on a one-dimensional periodic system, some of the conclusions are also applicable to two and three-dimension systems, though a separate investigation is required.

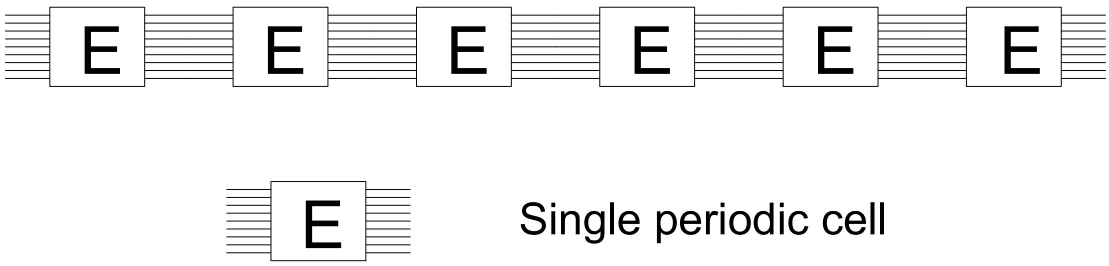

Figure 2.11. Multi-coupled one-dimensional periodic structure.

Another author who deals with multi-coupled one-dimension periodic structure is [A.Y.-T.Leung, 1980]. [A.Y.-T.Leung, 1980] gives a general idea about periodic structures. Among many subjects discussed in the paper, finite and infinite periodic systems and systems with periodic boundary conditions are presented. Furthermore a method for studying the natural vibration of periodic structures with multiple coupling is offered, where terms such as non-symmetric matrices and complex characteristic problem are avoided. The article presents a short theory about boundary forces and their relation to boundary displacements and internal displacement, and lastly the utilization of equation of motion through finite element in matrix form. In chapter three this theory will be clarified in details.

[Q. Gao and Williams, 2012] has written about one-dimension periodic structures and one-dimension periodic structures with defects. The article concentrates on presenting a method to compute the dynamic response of the periodic structures in question. The method is based on finding a detailed algorithm for computing the exponential of the the matrix corresponding to periodic structures. Taking advantage of symmetry in cells, many matrix elements became identical which leads to a simplification and less computational effort. Nevertheless further computational effort can be saved as there is energy propagation characteristic in the system. The article states, that the above two criteria make the method efficient and accurate.

In most of the studies above Floquet's theory was used in relation to periodic structures. Moreover finite element analysis have to be done in order to deal with most of the above-mentioned problems. These two problems will be described in details in chapter to and chapter three.

As it is seen above waves can be attenuated in many ways, whereas periodicity is one of the effective tools to solve the vibration problem. Nowadays there are many commercial software. Among these software COMSOL multiphysics is a software which is often used in this regard. In this project a commercial program COMSOL multiphysics is used to analyse different periodic structures. For verifying the results utilized by COMSOL, finite element program made in MatLab will be used simultaneously in computing simple cases.

Before digging deep into this program, the basic theory of finite elements in structural dynamics and vibration will be explained in the subsequent chapter.

3 Theory of finite elements in structural dynamics and vibrations

Application of dynamic analysis depends on whether the load is of higher frequency or applied suddenly. If the nature of loading is cyclic and has a frequency which is less than approximately one-quarter of the structure's lowest natural frequency, no dynamic analysis is needed, and the problem will be considered quasistatic. However if this is not the case then a dynamic analysis is necessary. The closer the frequency of loading is to a natural frequency of the structure the greater its magnitude will be. Therefore these two frequencies shall be well separated in order to avoid resonance. These frequencies and mode shapes can be determined from solving eigenvalue problem, which can also be used in solving problems related to buckling analysis. Presentation of eigenvalue problem is stated later in this chapter.

Apart from this, frequencies and modes are also used for calculation methods for harmonic responses. A harmonic analysis is a steady-state response or a response that repeats equal time intervals. A rotating machinery attached to the structure is an example of harmonic loading.

As mentioned above a suddenly applied load can also be considered dynamic. A time-varying response to this loading which is not periodic is through seeking the transient response or the response history. The solution for this type of loading is based on integration of differential equations of motion in time, for example the loading from earthquakes. One can also determine the maximum response of the suddenly applied non-periodic loading, which is through response spectrum analysis. Once again the vibration frequencies and modes of the structure shall be used together with the response history of a single-d.o.f. spring mass system subjected to the given time-varying of loading.

It shall be noticed that in all the above cases the external loading as a function of time shall be known [R.D. Cook, 1989].

In the following the some of the important parameters in dynamic analysis will be explained.

3.1 Dynamic equations. Mass and stiffness matrices

Single-d.o.f. System.

A typical example of a single-d.o.f. system is illustrated in the Figure 3.1. The system consists of a single mass m, single linear spring of stiffness k and a single viscous damper shown by dashpot. As it comes from its name, the damper has the job of damping the vibration, i.e. it applies resistance proportional to rate of deformation. In case of one-dimensional motion Newton's second law, $f = ma$ is applicable, where motion is a function of time $u = u(t)$ and governed by this Newton's second law. Likewise velocity can be described by $\dot{u} = du/dt$ and acceleration $a = \ddot{u} = d^2u/dt^2$. Having this in mind, Newton's second law can be stated as follow:

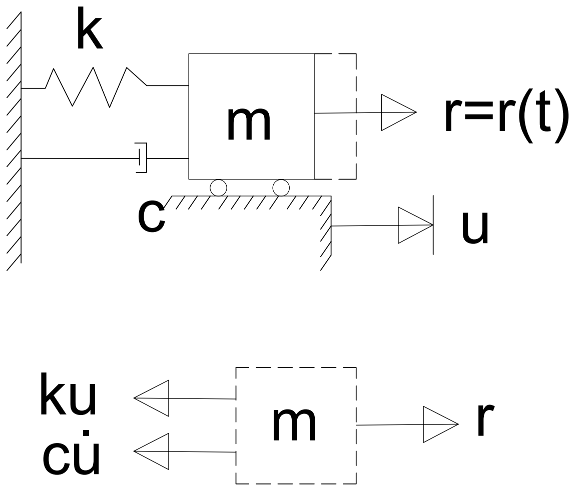

Figure 3.1. Single d.o.f. systems, with displaced configurations shown by dashed lines. Loading by time varying force r.

$$f = ma \qquad \Rightarrow \qquad r - ku - c\dot{u} = m\ddot{u} \qquad or \qquad m\ddot{u} + c\dot{u} + ku = r$$

$r = r(t)$	External load
ku	Internal force

In the following it will be illustrated how the governing equation for structural dynamics is derived for a multi d.o.f system.

3.1.1 Equation of motion for Multi d.o.f. system

Structural mass and damping are expressed by the governing equation for structural dynamics or the so-called equation of motion. The approach for this equation is shown in the following. The equation states that work done by external load is equal to the sum of work absorbed by inertial, dissipative, and internal forces for any virtual displacement. For a single element having a volume of V and surface area of S this work equilibrium is given as:

$$\begin{aligned} &\int \{\delta u\}^T\{F\}dV + \int \{\delta u\}^T\{\Phi\}dS + \sum_{i=1}^{n}\{\delta u\}_i^T\{p\}_i \\ &= \int \left(\{\delta u\}^T\rho\{\ddot{u}\} + \{\delta u\}^T c\{\dot{u}\} + \{\delta\epsilon\}^T\{\sigma\}\right) dV \end{aligned} \tag{3.1}$$

Here $\{\delta u\}^T$ and $\{\delta\epsilon\}^T$ can be written as $\{\delta u\}^T = \{\delta d\}^T[N]^T$ and $\{\delta\epsilon\}^T = \{\delta d\}^T[B]^T$
Where

$\{F\}$	Body force
$\{\Phi\}$	Surface traction
$\{p\}_i$	Prescribed concentrated load
$\{\delta u\}_i$	Virtual displacements $\quad \{\delta u\} = \lfloor \delta u \quad \delta v \quad \delta w \rfloor^T$
ρ	Mass density
c	Viscous damping parameter
$\{\delta\epsilon\}$	Strain corresponding to the displacement

According to finite element, discretization, displacement, velocity and acceleration can be written as follow

$$\begin{aligned} &\{u\} = [N]\{d\} \quad \{\dot{u}\} = [N]\{\dot{d}\} \quad \{\ddot{u}\} = [N]\{\ddot{d}\} \quad where \quad \{u\} = \lfloor u \quad v \quad w \rfloor^T \\ &\{\epsilon\} = [B]\{d\} \qquad\qquad where \qquad [B] = [\partial][N] \end{aligned} \tag{3.2}$$

In 3.2 $[B]$ is the strain-displacement matrix and $\{d\}$ lists the nodal displacement d.o.f. Here the shape functions $[N]$ are functions of space and the nodal d.o.f. $\{d\}$ are functions of time.

Combining equation (3.1) and (3.2) and assuming the concentrated load $\{p\}_i$ are located at nodes, the following is obtained.

$$\{\delta d\}^T \left[\int \rho \, [N]^T \, [N] \, dV \{\ddot{d}\} + \int c \, [N]^T \, [N] \, dV \{\dot{d}\} \right. \tag{3.3}$$
$$\left. + \int [B]^T \, \{\sigma\} dV - \int [N]^T \, \{F\} dV - \int [N]^T \, \{\Phi\} dS - \sum_{i=1}^{n} \{p\}_i \right] = 0$$

The first term in equation (3.3) is the element mass matrix, the second term is related to the damping matrix.

$$[m] = \int \rho [N]^T [N] dV \qquad\qquad [c] = \int c[N]^T [N] dV \tag{3.4}$$

The third term in equation (3.3) is known as the internal force vector $\{r^{int}\}$

$$\{r^{int}\} = \int [B]^T \{\sigma\} dV \tag{3.5}$$

The last three terms in equation (3.3) illustrates the external load.

$$\{r^{ext}\} = \int [N]^T \, \{F\} dV + \int [N]^T \, \{\Phi\} dS + \sum_{i=1}^{n} \{p\}_i \tag{3.6}$$

Rearranging from equation (3.4) through (3.6) a balance between internal and external forces can be arranged, where equation (3.3) yields.

$$[m]\{\ddot{d}\} + [c]\{\dot{d}\} + \{r^{int}\} = \{r^{ext}\} \tag{3.7}$$

In case the material is linearly elastic, then the internal load associated with element stresses are $\{r^{int}\} = [k]\{d\}$, where $[k]$ denotes the conventional element stiffness matrix. Replacing this back in (3.7), the following is obtained.

$$[m]\{\ddot{d}\} + [c]\{\dot{d}\} + [k]\{d\} = \{r^{ext}\} \tag{3.8}$$

It shall be noted that equation (3.8) is also applicable for nonlinear material properties.

The global form of equation (3.7) and (3.8) are symbolized by capital letters as follow:

$$[M]\{\ddot{D}\} + [C]\{\dot{D}\} + \{R^{int}\} = \{R^{ext}\} \tag{3.9}$$
$$[M]\{\ddot{D}\} + [C]\{\dot{D}\} + [K]\{D\} = \{R^{ext}\} \tag{3.10}$$

The equations show that internal forces which are combined of inertial forces, damping forces and internal stresses equilibrates the external forces. As the case in this project is without damping therefore the middle term in (3.10) disappears and this equations takes the following shape [R.D. Cook, 1989].

$$\boxed{[M]\{\ddot{D}\} + [K]\{D\} = \{R^{ext}\}} \tag{3.11}$$

In the following mass matrix and stiffness matrix for bar- and beam element are presented in Figure 3.2.

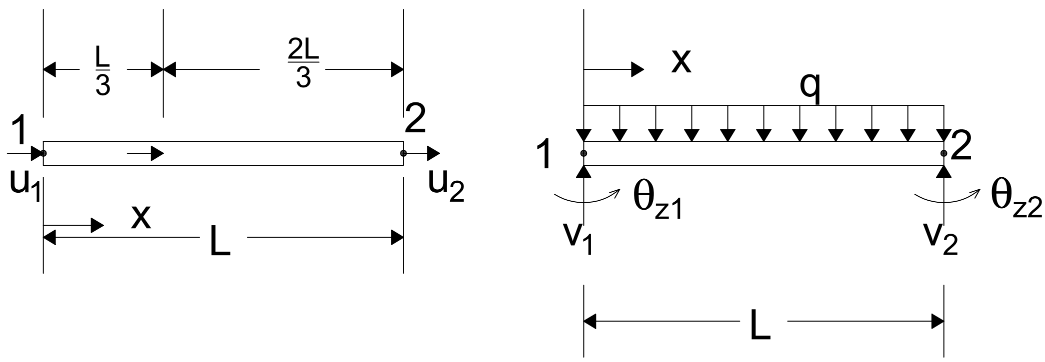

Figure 3.2. Uniform bar element with concentrated load P at one-third of the beam (left). Uniform beam element with uniformly distributed downward load of q (right).

It shall be noticed that the procedure for both beam and solid are the same.

3.1.2 Lumped mass matrix and consistent mass matrix

Two kind of mass matrices will be discussed in the following, lumped mass matrix, and consistent mass matrix. *" A mass matrix is a discrete representation of a continuous mass distribution"* [R.D. Cook, 1989] The difference between these two types of matrices lies in their diagonal, where lumped mass matrix is diagonal and consistent mass matrix is not. Depending on the outcome of a procedure, one or the other matrix may be a best fit. In some cases a combination of both even gives a better solution. Since lumped mass matrix is a diagonal matrix, therefore in some cases it has the advantage of using less computational space.

Lumped mass matrix

For a two-node bar element shown in Figure 3.3a with the total mass of $m = \rho AL$, where L is the length, ρ the mass density and A is the cross-sectional area, the mass will be divided in two, with $m/2$ at each node. This leads to a discontinuous displacement field as shown in Figure 3.3a where the two halves of the element translates separately. The lumped element mass matrix for this element with mass m and the corresponding inertia forces associated with nodal acceleration $\ddot{u}_1$ and $\ddot{u}_2$ can be written as follow.

$$[m] = \frac{m}{2}\begin{bmatrix} 1 & 0 \\ 0 & 1 \end{bmatrix} \qquad \Rightarrow \qquad [m]\left\{ \begin{array}{c} \ddot{u}_1 \\ \ddot{u}_2 \end{array} \right\} = \left\{ \begin{array}{c} F_1 \\ F_2 \end{array} \right\} \tag{3.12}$$

In presence of rotational d.o.f. in element, an extra factor shall be add, as this rotational inertia is not included in mass particles.

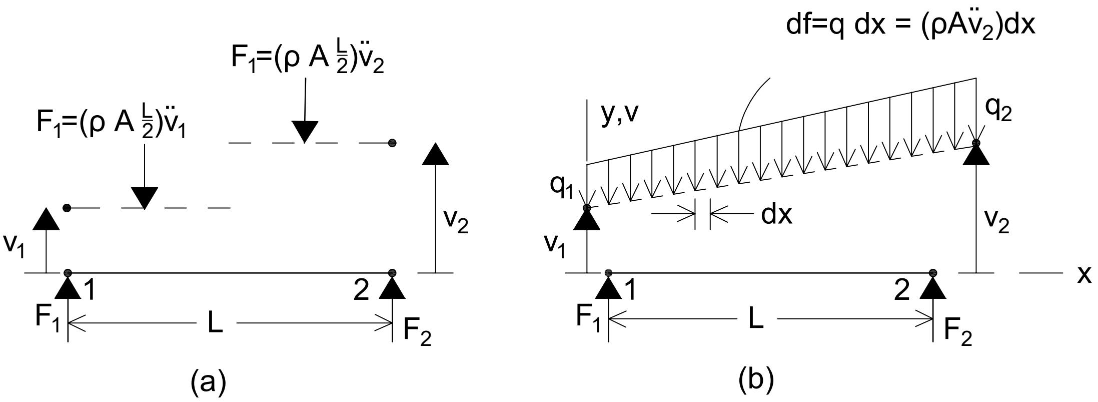

Figure 3.3. Lateral displacements of a two-node bare element are shown by dashed lines. (a) Implied by ad hoc lumping. F_1 and F_2 are inertia forces. (b) Linear displacement field provides the consistent [m] of a bar element.

Consistent mass matrix

Contrary to mass matrix for the same two-node bar element in Figure 3.3b the displacement is linear in the axial coordinate. For a lateral displacement in y-direction as in Figure 3.3b with mass $m = \rho AL$, the following can be obtained from equation (3.4). The corresponding shape functions for a bar-elements can be seen in the following Figure 3.4

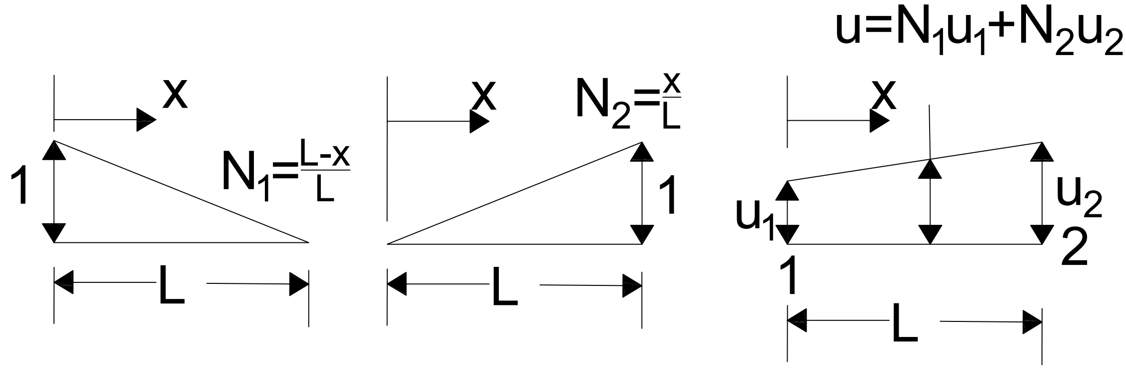

Figure 3.4. Shape function (N^{bar}) for a bar element.

$$[N^{bar}] = \left\lfloor \frac{L-x}{L} \right\rfloor \qquad [m^{bar}] = \int_0^L [N]^T[N^{bar}]\rho A dx = \frac{m}{6}\begin{bmatrix} 2 & 1 \\ 1 & 2 \end{bmatrix} \tag{3.13}$$

which operates on a nodal acceleration vector $\{\ddot{d}\} = \lfloor \ddot{u}_1 \quad \ddot{u}_2 \rfloor^T$. Accordingly for a two node beam element with d.o.f. $\{d\} = \lfloor v_1 \quad \theta_{z1} \quad v_2 \quad \theta_{z2} \rfloor^T$ the consistent mass matrix is constructed as follow:

$$[m^{beam}] = \int_0^L [N]^T[N^{beam}]\rho A dx = \frac{m}{420}\begin{bmatrix} 156 & 22L & 54 & -13L \\ 22L & 4L^2 & 13L & -3L^2 \\ 54 & 13L & 156 & -22L \\ -13L & -3L^2 & -22L & 4L^2 \end{bmatrix} \tag{3.14}$$

The corresponding shape functions $[N^{beam}]$ in equation 3.14 for a beam element in Figure 3.2 are presented in Figure 3.5 [1].

[1] In case the beam element stiffness matrix takes transverse shear deformation in to account, the shape functions differ. For more information refer to [R.D. Cook, 1989]

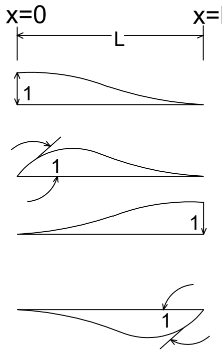

	At x=0		At x=L	
	N_i	$N_{i,x}$	N_i	$N_{i,x}$
$N_1=1-3x^2/L^2+2x^3/L^3$	1	0	0	0
$N_2=x-2x^2/L+x^3/L^2$	0	1	0	0
$N_3=3x^2/L^2+2x^3/L^3$	0	0	1	0
$N_4=x^2/L^2+x^3/L^3$	0	0	0	1

Figure 3.5. Shape function (N^{beam}) for a beam element.

3.1.3 Element stiffness matrix

In this section element stiffness matrices for both bar- and beam element will be presented. For a two d.o.f. bar element and a four d.o.f. beam element in Figure 3.6 for a static problem. The relationship between force and displacement is as follows.

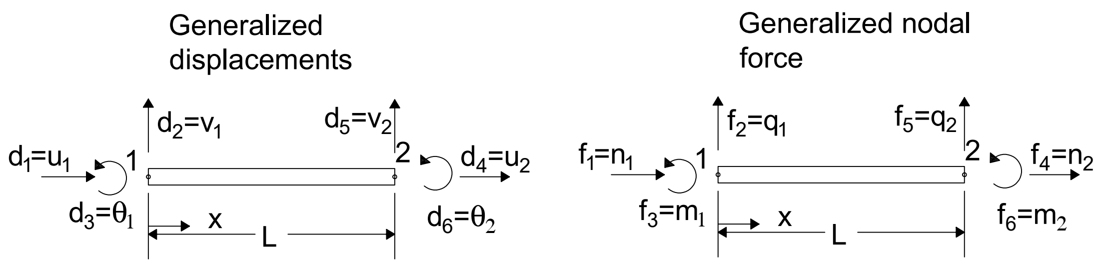

Figure 3.6. Generalized displacement and generalized nodal force.

$$[k]^{bar}\begin{Bmatrix} u_1 \\ u_2 \end{Bmatrix} = \begin{Bmatrix} n_1 \\ n_2 \end{Bmatrix} \qquad [k]^{bar}\begin{Bmatrix} d_1 \\ d_4 \end{Bmatrix} = \begin{Bmatrix} f_1 \\ f_4 \end{Bmatrix} \tag{3.15}$$

$$[k]^{beam}\begin{Bmatrix} v_1 \\ \theta_1 \\ v_1 \\ \theta_2 \end{Bmatrix} = \begin{Bmatrix} q_1 \\ m_2 \\ q_1 \\ m_2 \end{Bmatrix} \qquad [k]^{beam}\begin{Bmatrix} d_2 \\ d_3 \\ d_5 \\ d_6 \end{Bmatrix} = \begin{Bmatrix} f_2 \\ f_3 \\ f_5 \\ f_6 \end{Bmatrix} \tag{3.16}$$

The stiffness matrices in dynamic analysis are exactly the same as the stiffness matrices used static analysis. Matrices in (3.17) shows stiffness matrices for bar element with only axial displacements at nodes, and equation (3.18) shows beam element which operates on $\{d\} = \lfloor v_1 \quad \theta_1 \quad v_2 \quad \theta_2 \rfloor^T$

$$Bar : [k^{bar}] = \begin{bmatrix} \frac{AE}{L} & -\frac{AE}{L} \\ -\frac{AE}{L} & \frac{AE}{L} \end{bmatrix} \tag{3.17}$$

$$Beam : [k^{beam}] = \begin{bmatrix} \frac{12EI_z}{L^3} & \frac{6EI_z}{L^2} & \frac{-12EI_z}{L^3} & \frac{6EI_z}{L^2} \\ \frac{6EI_z}{L^2} & \frac{4EI_z}{L} & \frac{-6EI_z}{L^2} & \frac{2EI_z}{L} \\ \frac{-12EI_z}{L^3} & \frac{-6EI_z}{L^2} & \frac{12EI_z}{L^3} & \frac{-6EI_z}{L^2} \\ \frac{6EI_z}{L^2} & \frac{2EI_z}{L} & \frac{-6EI_z}{L^2} & \frac{4EI_z}{L} \end{bmatrix} \tag{3.18}$$

Combining (3.17) and (3.18) delivers the combined stiffness matrix for bar and beam elements formed in the following manner

$$[k] = \begin{bmatrix} \frac{AE}{L} & 0 & 0 & -\frac{AE}{L} & 0 & 0 \\ 0 & \frac{12EI_z}{L^3} & \frac{6EI_z}{L^2} & 0 & \frac{-12EI_z}{L^3} & \frac{6EI_z}{L^2} \\ 0 & \frac{6EI_z}{L^2} & \frac{4EI_z}{L} & 0 & \frac{-6EI_z}{L^2} & \frac{2EI_z}{L} \\ -\frac{AE}{L} & 0 & 0 & \frac{AE}{L} & 0 & 0 \\ 0 & \frac{-12EI_z}{L^3} & \frac{-6EI_z}{L^2} & 0 & \frac{12EI_z}{L^3} & \frac{-6EI_z}{L^2} \\ 0 & \frac{6EI_z}{L^2} & \frac{2EI_z}{L} & 0 & \frac{-6EI_z}{L^2} & \frac{4EI_z}{L} \end{bmatrix}$$

3.2 Natural frequencies and modes

Undamped multiple-d.o.f. free vibration

In absence of damping, movement of all d.o.f. are in phase with each other at the same frequency ω i.e. load r illustrated in Figure 3.1 is zero and the motion is described by $u = \bar{u} \sin \omega t$. The cyclic frequency is $f = \omega/2\pi$ and a period is defined as $T = 1/f$.

Where:

$\bar{u}$	Amplitude of vibration
ω	Circular frequency $[\frac{rad}{s}]$
f	Cyclic frequency [Hertz; cycles per second)]
T	Periods [seconds]

Vibratory motion consists of nodal amplitudes $\{\bar{D}\}$. These amplitudes vary sinusoidally with time relative to static equilibrium displacements $\{D_{st}\}$ which is produced by time-independent loads. It shall be noted that in case of a linear problem natural frequencies are independent of $\{D_{st}\}$ where the nonstructural mass associated with the static loads must still be represented in $[M]$.

Vibration that produces nodal displacements and accelerations are:

$$\{D\} = \{\bar{D}\}\sin\omega t \qquad \{\ddot{D}\} = -\omega^2\{\bar{D}\}\sin\omega t \tag{3.19}$$

Under the condition where damping matrix $[C]$ disappears equation (3.8) and (3.19) yields the following

$$\left(\{K\} - \omega^2\{M\}\right)\{\bar{D}\} = \{0\} \tag{3.20}$$

Above equation (3.20) is the eigenproblem equation

where

ω^2	An eigenvalue
ω	A natural frequency
$\{K\} - \omega^2\{M\}$	Dynamic stiffness matrix

To better understand the physical meaning of vibration equation (3.20) can be rewritten as $\{K\}\{\bar{D}\} = \omega^2\{M\}\{\bar{D}\}$ which tells that in a vibration mode elastic resistances are in balance with inertia loads. If there is a non-trivial solution to exist then the determinant of $\{K\} - \omega^2\{M\}$ has to give zero.

In the following, the above-mentioned theory is illustrated through two simple examples of a beam with different boundary conditions. The first condition is a fixed-fixed beam and the second one is a free-free beam.

3.2.1 Natural frequencies of a fixed-fixed and free-free beam

Two similar beams with different boundary conditions of clamped-clamped and free-free are analysed in the following. Apart from the the different boundary conditions the beams have the exact same geometry and properties. The beams in question have a solid rectangular cross section with the following properties.

Table 3.1. Properties of the beams.

Youngs modulus E	$210 \times 10^9\,\mathrm{Pa}$
Poisson's ratio μ	0,3 –
Density ρ	$7860\,\mathrm{kg/m^3}$
Length L	1,2 m
Cross section height h	0,015 m
Cross section width w	0,015m
Second moment of area I	$4{,}2190 \times 10^{-9}\,\mathrm{m^4}$

The analysis is done in two commercial softwares, MatLab and COMSOL multiphysics. Thereafter the results from these two programs will be compared and discussed. Before extracting the natural frequencies of the beam, a convergence analysis is done in order to determine adequate number of elements for calculating the eigenmodes as precise as possible.

Natural frequencies of beam with clamped-clamped boundary conditions

The beam is analysed in two different models in COMSOL, in Bezier polygon shown in Figure 3.7 and in solid model shown in Figure 3.9. Bezier polygon corresponds to the beam model in MatLab This makes perfect sense as in the Figure 3.7 the structure is shown as a line i.e. both MatLab and Bezier polygon defines the geometry in two-dimensions. Whether Bezier polygon is used under the physics of "beam" or "solid" does not makes any difference. The only difference is some of the limitations shown in Table 3.2.

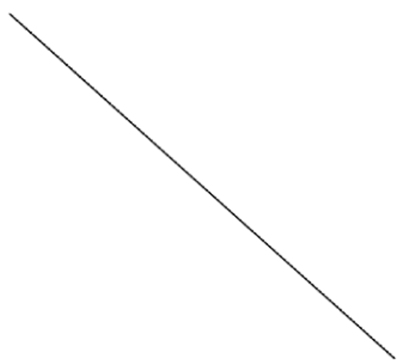

Figure 3.7. Beam build in a Bezier polygon.

The geometries are chosen under the physics of "Structural Mechanics" and then "Solid Mechanics (solid)" for a three-dimensional structure and "beam" for a two-dimensional structure. The difference between these physics can be better illustrated in the following Table.

Table 3.2. Illustration of differences between the different models used in COMSOL.

Model Wizard 3D		
	Beam(beam)	Solid Mechanics (solid)
Bezier polygon 2D	All types of boundary conditions are availible here except periodic boundary conditions	Boundary conditions can not be applied to structures here
Solid 3D	Periodic boundary conditions can not be applied here	All types of boundary conditions are applicable here including periodic boundary conditions

In above Table 3.2 note that "Model Wizard 3D" on top of the Table means that the geometry can be rotated in three dimensions and not necessary a three-dimensional geometry, in case it was stated 2D then the geometry would only be able to rotate in in two-dimensions.

The following Figure 3.8 illustrates the convergence analysis for Bazier polygon.

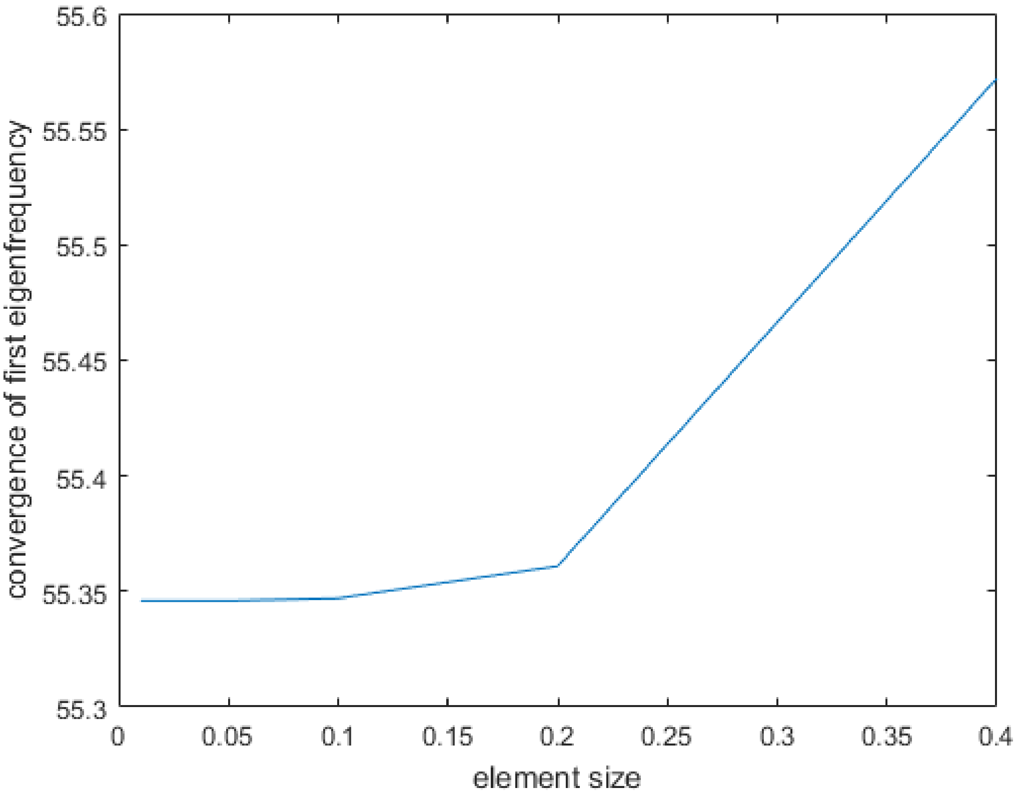

Figure 3.8. Convergence analysis for beam model in COMSOL and MatLab.

The Figure above in 3.8 illustrates the convergence analysis of first eigenfrequency. The Figure is plotted based on the following values.

Table 3.3. Convergence analysis.

COMSOL element size	MatLab element size	First eigenfrequency
0,40 m	0,40 m	55,572 Hz
0,20 m	0,20 m	55,361 Hz
0,10 m	0,10 m	55,347 Hz
0,05 m	0,05 m	55,346 Hz
0,01 m	0,01 m	55,346 Hz

As it is seen in tabel 3.3 the first eigenmode is converged equally in both programs (MatLab and COMSOL), therefore in Figure 3.8 the first mode was considered sufficient to represent the convergence analysis. Furthermore it is shown that the values from Matlab are exactly the same as in COMSOL, therefore Figure 3.8 can represent the convergence analysis for the corresponding beam in MatLab as well.

As it is demonstrated in case of Bezier's polygon the beam has converged with an element size of 0,05 m. Similarly the beam was tested in a solid model seen in figure 3.9 [2]

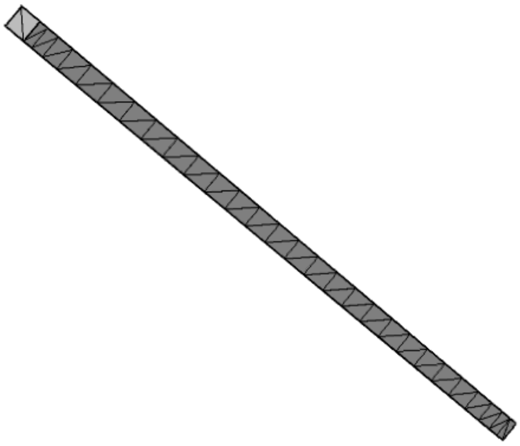

Figure 3.9. Beam build in a solid geometry.

Again a convergence analysis was done in order to find the appropriate element size, so thereby the results are as accurate as possible. The results of convergence are demonstrated below in Tabel 3.4 and Figure 3.10

Table 3.4. Convergence analysis in a solid geometry .

COMSOL element size	First eigenfrequency
0,109 m	56,161 Hz
0,096 m	55,906 Hz
0,048 m	55,632 Hz
0,024 m	55,540 Hz
0,012 m	55,378 Hz
0,006 m	55,363 Hz
0,003 m	55,355 Hz

The corresponding convergence plot based on the above Table 3.4 is plotted below.

[2]The mesh shown in Figure 3.9 is only viewed for demonstration purpose.

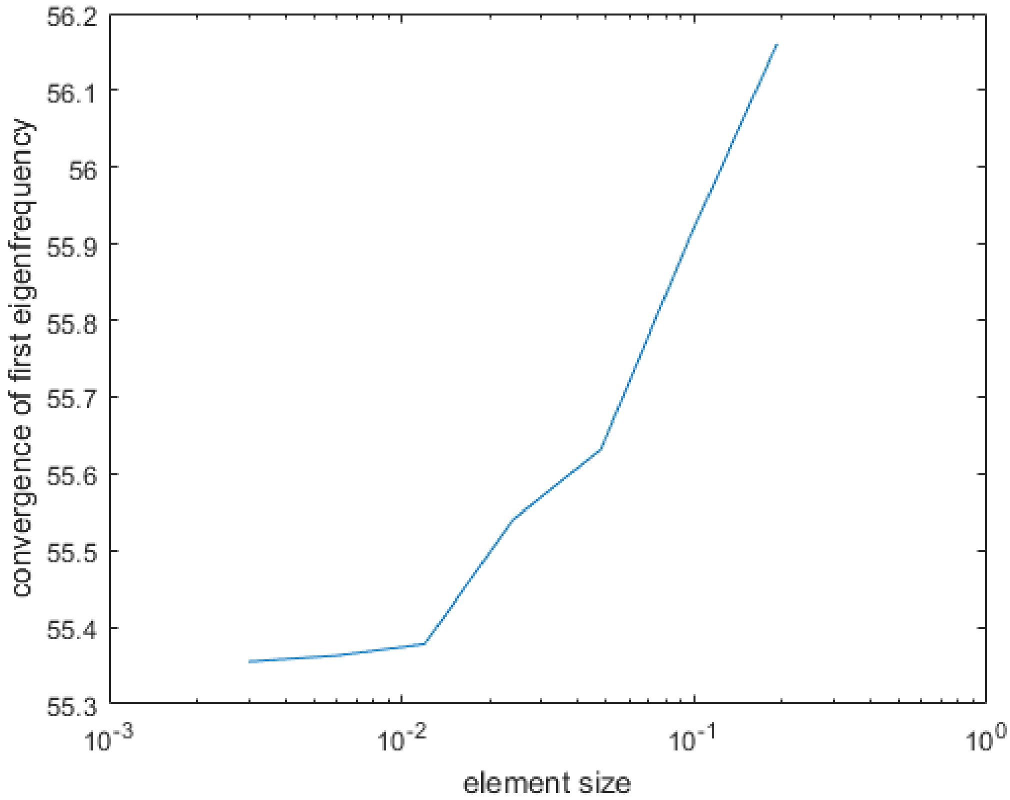

Figure 3.10. Convergence analysis for a solid geometry.

As it is seen above the convergence for the solid geometry has not stopped yet and even for an element size of 0,003 m the convergence still continues. Due to time consumption and computational memory, it was decided to stop the convergence at this point.

Choosing a proper element size is very important in finite element analysis. As stated in [Andersen, 2006]"the element size, is defined by the shortest wavelength in the system." The order of interpolation determines the number of element, for an accurate numerical results. the minimum number of elements for a linear interpolation is 10 to 12 elements per wave. For a quadratic interpolation four to five elements are needed per wave length and for a cubic interpolation two to three elements per wave are needed.

The final results for the convergence analysis are as follow:

Table 3.5. Final element size for convergence analysis.

	COMSOL Solid	COMSOL Bezier polygon	MatLab
Element size	0,003 m	0,05 m	0,05 m
First eigenfrequency	55,355 Hz	55,346 Hz	55,346 Hz

Based on the convergence analysis it is determined to use the results from Table 3.5 as a final number of elements for determining the natural frequencies.

The first 10 modes from beam model in COMSOL and MatLab with fixed-fixed boundary conditions can be seen below.

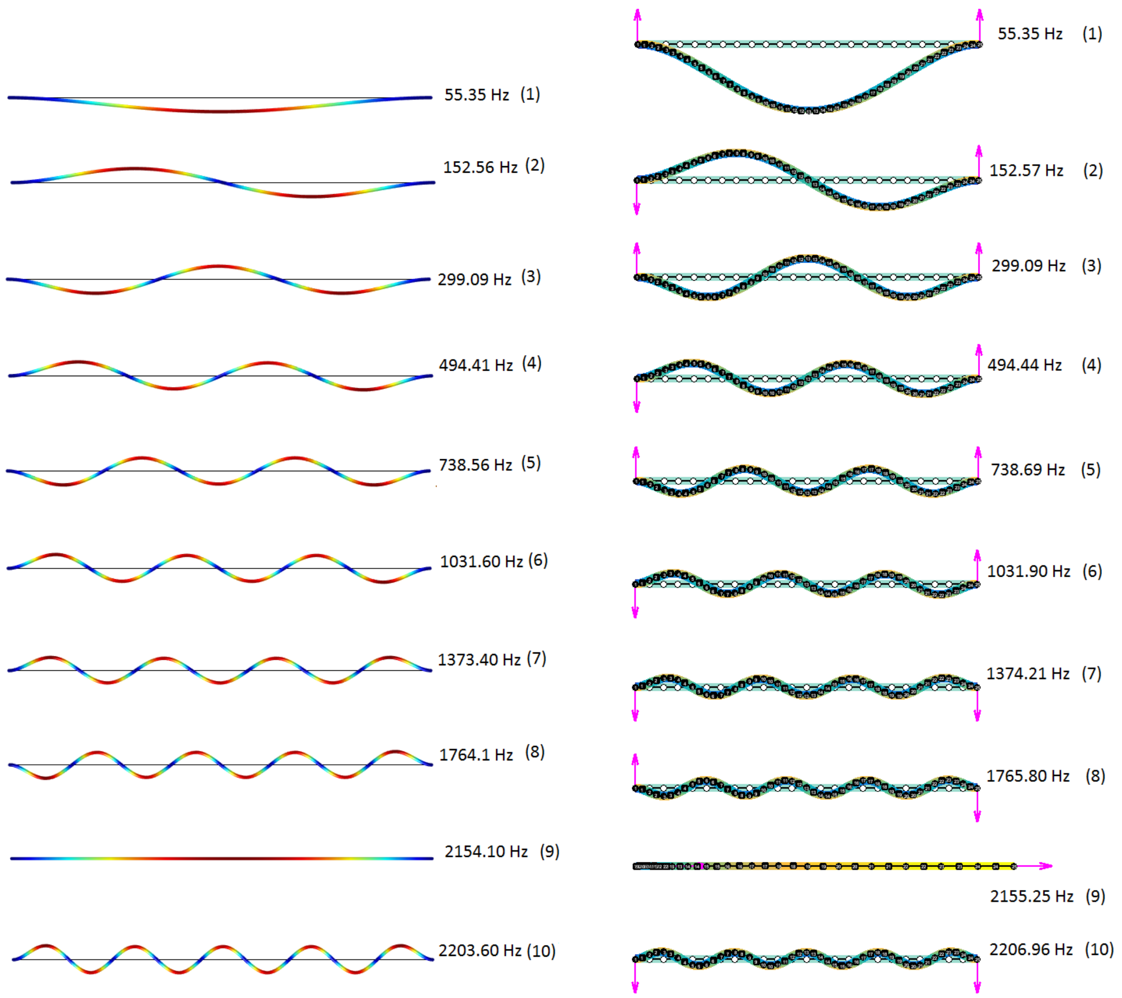

Figure 3.11. The first 10 eigenmodes for the beam in Bezier polygon on the left and MatLab on the right.

The colours in the Figure 3.11 left shows the deformation, where blue shows the least value and red shows the highest deformation. Whereas the arrows in MatLab shows the reaction. Pay attention to mode 9 in the above Figure 3.11. This mode is torsional, as the boundary condition is fixed on both ends it is not visible. This mode is better illustrated on the right in three-dimension version of the COMSOL.

Now the first 10 modes will be analysed in a solid geometry and afterwards it will be fair to compare it with the results from Bezier polygon, as both models are built in COMSOL. The 10 eigenmodes are illustrated in the following.

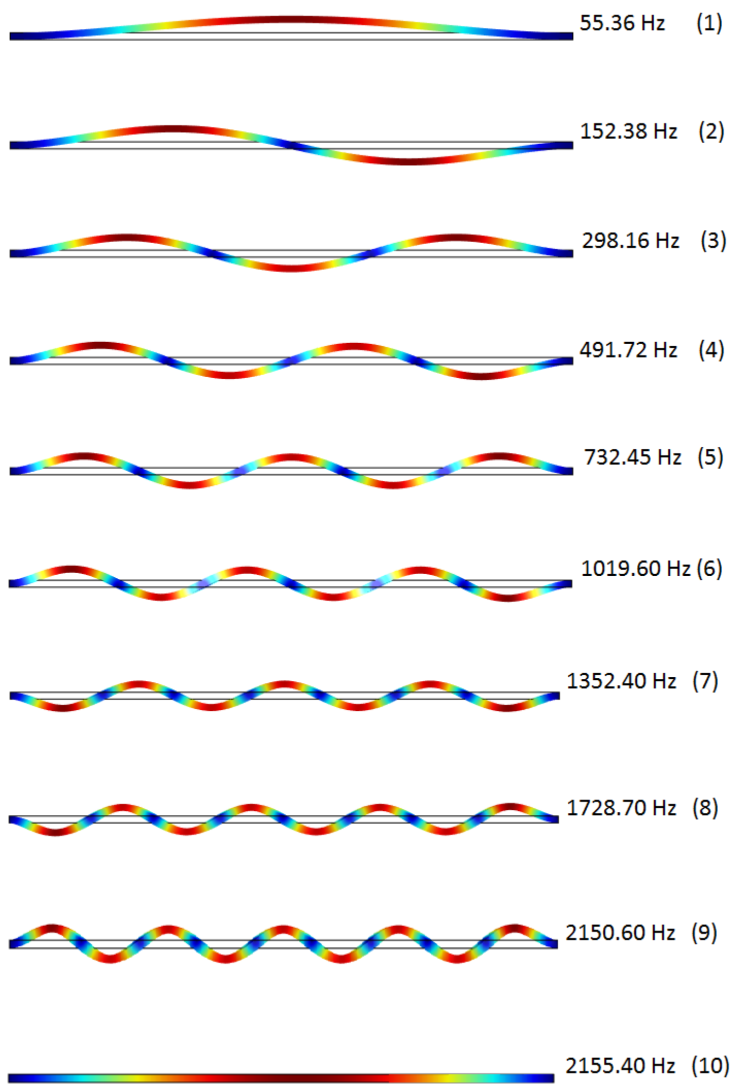

Figure 3.12. The first 10 eigenmodes for a solid geometry.

An obvious difference lies in mode 10th in Figure 3.12 which is the same as mode nine in Figure 3.11, this is due to the fact that torsional modes shown below in Figure 3.13 are not listed in Figure 3.12. The COMSOL And MatLab files are in the appendix CD in the folder of "Beam".

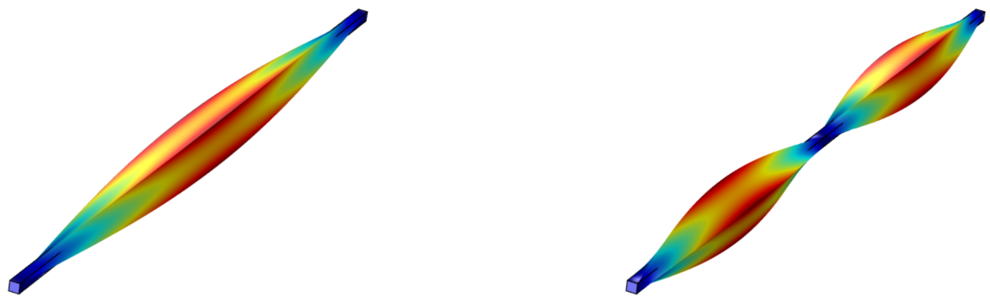

Figure 3.13. Axial and torsional modes.

As seen the modes in Figure 3.13 are torsional. The reason for not including them in the Figure 3.12 is only for comparison reason, as such modes can not appeared in two-dimension and therefore the comparison will be confusing, therefore this specific mode appears in 10th position.

As the modes for a beam with fixed-fixed boundary conditions are demonstrated, it will be interesting to know how a beam with free-free boundary conditions behaves in the aforementioned two programs.

Natural frequencies of a beam with free-free boundary conditions

In this section the same analysis will be done as previous. As the geometry of the beam remains the same, therefore no convergence analysis will take place. Again the beam in question will be analysed in Matlab and COMSOL where the above-mentioned models (Bezier polygon and solid) will be used. The results will be then plotted, compared and discussed.

The first 10 modes of beam with free-free boundary conditions are shown below in Figure 3.14

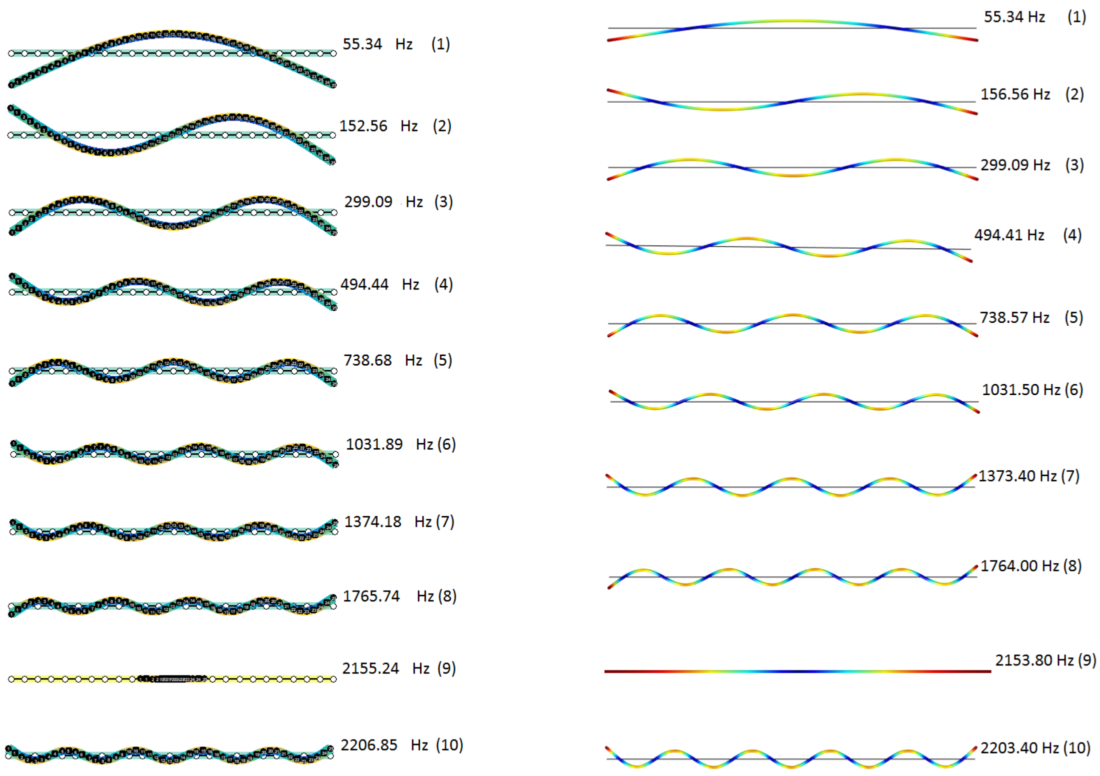

Figure 3.14. The first 10 eigenfrequencies with free-free boundary condition. COMSOL to the right and MatLab to the left.

Clearly the difference between the MatLab version and COMSOL (Bezier polygon) starts at mode four, as a change in decimals appears. An apparent reason according to COMSOL user guide is that COMSOL modifies the shape functions for Timoshenko case (which is used in this case), so that they depend on the degree of shear flexibility. This can be seen in COMSOL under "Model Builder" "Linear Elastic Material" and then equations in the appendix file $C\_C\_1.2m\_0.015m\_rec\_polygon\_3D$. Again mode nine appears to be axial in Figure 3.14. All other modes behave as expected and nothing different is seen in these modes.

Now once again a solid model will be used to extract the eigenfrequencies. It is expected that again the modes from COMSOL will be similar to the ones from MatLab. As previous the solid model will be compared with Bezier polygon in COMSOL. The first 10 eigenfrequencis in solid models are illustrated below.

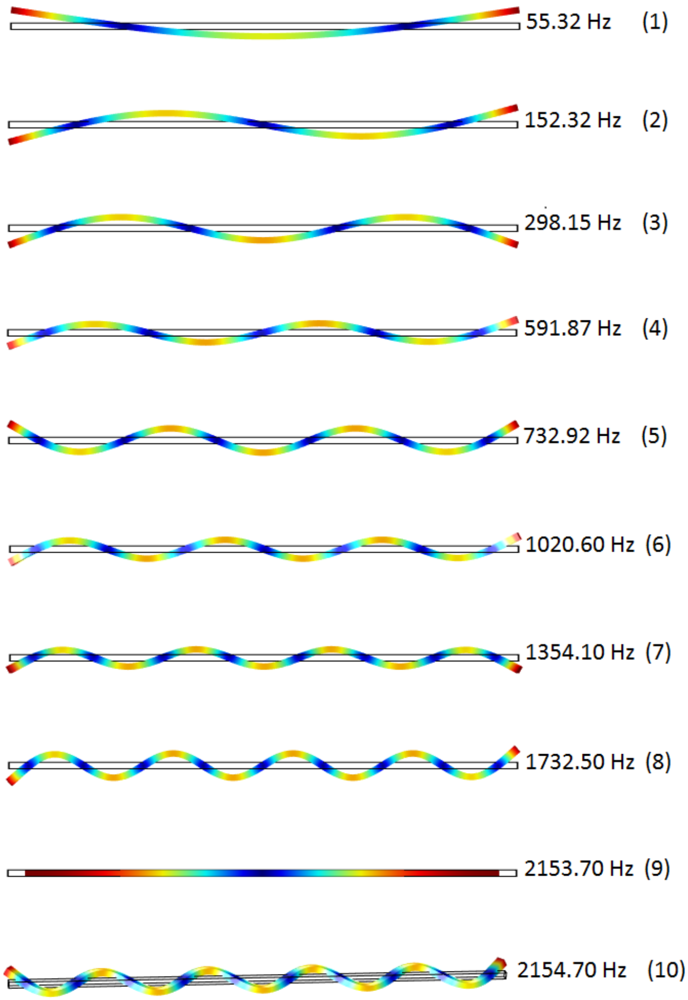

Figure 3.15. The first ten modes in solid model in COMSOL.

It shall be emphasized that again only the modes that are comparable in both programmes are shown here and a torsional mode as in Figure 3.16 is not added here. As expected mode nine is again an axial mode. Since the boundaries are free at both ends it is clearly demonstrated that the mode is axial, as the beam is contracted from both ends. Interestingly the difference in Hz between mode nine and ten is not too big.

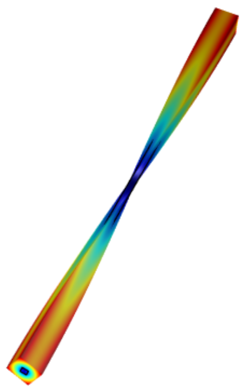

Figure 3.16. The first 10 eigenmodes for a solid geometry.

3.2.2 Discussion of results

As it is demonstrated above in case of a simple problem both MatLab and COMSOL (Bezier polygon) give a good result up to fourth mode. Again the same reason as previous is applicable here, which is due to the modification of shape functions according to Timoshenko's theory.

In case of solid model, the main problem was convergence, as a full convergence did not happen. Therefore the precession of the results from solid geometry can not be decided. In case there is enough computational capacity, a full convergence analysis can be done and a more accurate result can be obtained. Solid model has benefits in many cases. One of the benefits observed through analysis was depiction of modes in Figures 3.16 and 3.13. A 3D model gives a clear illustration of such modes, which are impossible to see in other models for example in 2D models. Even though a full convergence did not happen still the 3D geometry gave smaller values compared to the other models. Another benefit of solid model is, the geometry is built as it is in reality, thus its behaviour will also be much realistic compared to 2D in Bezier polygon.

Another major difference lies in the illustration of double modes, i.e. a same mode in two different directions, which is the case in a 3D model. This will not be possible in 2D model.

Through analysis it was discovered that the way COMSOL deals with a beam model, which corresponds to MatLabs beam model was through Bezier's polygon. As it was also shown that Bezier's polygon gives almost the exact same results as MatLab as both models in both cases are *beam*. It shall be noted that Bezier polygon can be chosen under either physics "beam" or "solid", as it performs the same task in both physics, though it is a good idea to choose the Bezier polygon in the physics of "beam" in COMSOL, as more functions will be enabled. The Bezier polygon can also be chosen in the physics of "Solid" but many functions will be either not available or simply not enable to use as shown in Table 3.2.

As the idea of extracting the natural frequencies of a beam is clear, now the natural frequencies of a simple periodic structure will be extracted. In this particular case the periodic structure is a beam made of periodic cells, where a single cell will be analysed

4 Periodicity in structures

According to Chapter 2, periodic structures can be useful in attenuation of vibration. In order to tackle this problem, one would think that all the cells in a periodic structure have to be studied in regard to the propagation of waves. Gaston Floquet, a French mathematician, demonstrated that only one unit cell from the periodic structure is sufficient to study a particular periodic structure. For better understanding of this mathematical concept, Floquet's theory is presented in the following chapter.

The chapter is mainly build of three parts. The first part starts by theory, where Floquet's theory and finite elements analysis of a periodic structure is explained. The second part deals with a one-dimensional periodic cell built in COMSOL and MatLab where the results are compared. The third part of the chapter deals with a complex geometry build in COMSOL where Floquet's boundary conditions are used.

4.1 Finite element analysis of periodic structures

4.1.1 Cell dynamics

At a frequency ω the dynamic equation of a cell obtained from the FE model is

$$(K + \omega^2 M)q = f \tag{4.1}$$

As previously mentioned, damping will not be taken into consideration in this project, therefore the term related to damping is not included in equation (4.1). In the above equation K and M denotes stiffness and mass matrices, f denotes the loading vector q denotes the degrees of freedom vector.

Assuming that no external forces act on the internal nodes, the dynamic stiffness matrix $\tilde{\mathbf{D}} = \mathbf{K} - \omega^2\mathbf{M}$ takes the following form.

$$\begin{bmatrix} \tilde{D}_{II} & \tilde{D}_{IL} & \tilde{D}_{IR} \\ \tilde{D}_{LI} & \tilde{D}_{LL} & \tilde{D}_{LR} \\ \tilde{D}_{RI} & \tilde{D}_{RL} & \tilde{D}_{RR} \end{bmatrix} \begin{bmatrix} q_I \\ q_L \\ q_R \end{bmatrix} = \begin{bmatrix} 0 \\ f_L \\ f_R \end{bmatrix} \tag{4.2}$$

In above equation (4.2) the dynamic stiffness matrix is decomposed in three groups, left (L), Right (R) and interior (I) degrees of freedom.

In order to relate the generalized forces and displacements at left (L) and Right (R) nodes of the cell, the internal nodes in equation (4.2) will be condensed by using the first row of (4.2) as follow:

$$q_I = -\tilde{D}_{II}^{-1}(\tilde{D}_{IL}q_L + \tilde{D}_{IR}q_R). \tag{4.3}$$

Which will lead to

$$\begin{bmatrix} \tilde{D}_{LL} - \tilde{D}_{LI}\tilde{D}_{II}^{-1}\tilde{D}_{IL} & \tilde{D}_{LR} - \tilde{D}_{LI}\tilde{D}_{II}^{-1}\tilde{D}_{IR} \\ \tilde{D}_{RL} - \tilde{D}_{RI}\tilde{D}_{II}^{-1}\tilde{D}_{IL} & \tilde{D}_{RR} - \tilde{D}_{RI}\tilde{D}_{II}^{-1}\tilde{D}_{IR} \end{bmatrix} \begin{bmatrix} q_L \\ q_R \end{bmatrix} = \begin{bmatrix} f_L \\ f_R \end{bmatrix} \tag{4.4}$$

Where after partitioning

$$q = \begin{bmatrix} q_L \\ q_R \end{bmatrix} \qquad and \qquad f = \begin{bmatrix} f_L \\ f_R \end{bmatrix}$$

Which can also be written in the following form

$$\begin{bmatrix} D_{LL} & D_{LR} \\ D_{RL} & D_{RR} \end{bmatrix} \begin{bmatrix} q_L \\ q_R \end{bmatrix} = \begin{bmatrix} f_L \\ f_R \end{bmatrix} \tag{4.5}$$

Where

$$\begin{bmatrix} D_{LL} & D_{LR} \\ D_{RL} & D_{LR} \end{bmatrix} = [K - \omega^2 M] \tag{4.6}$$

4.1.2 Wave finite element for one-dimensional structural waveguides

The motion of a cell at any circular frequency ω is equal to $e^{-i\mu}$ times that of its neighbor, where $\mu = kL$ is called propagation constant, k is the wavenumber and L is the length of cell. The curves which give the relation between the propagation constant μ and the circular frequency ω, are called the dispersion curves. These curves describe the behaviour of an infinite periodic structure.

Looking back at the cell displacement vector in equation (4.5), Floquet's theorem states that the displacements on left and right side of the a cell can be shown by following equation (4.7)

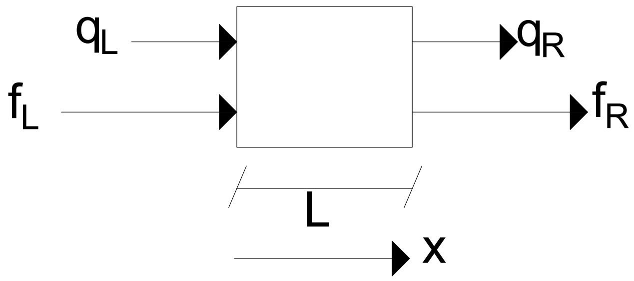

Figure 4.1. Unit-cell with force and displacement vectors shown on both sides.

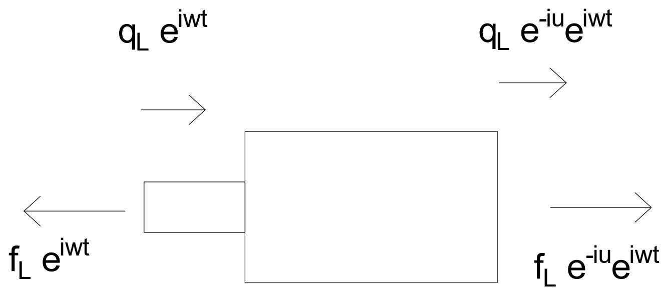

Figure 4.2. Schematic representation of displacements and forces at the ends of a unit cell.

$$\{q_R\} = \lambda\{q_L\} \tag{4.7}$$

where $\lambda = e^{(-i\mu)}$. Applying the periodicity condition, the following can be written

$$q = [\Lambda_R]q_L \qquad where \qquad [\Lambda_R] = [I \quad \lambda I]^T \tag{4.8}$$

where I is the identity matrix of the same dimension as q_L. Forces are handled the same way as $f = [f_L^T \quad f_R^T]^T$. As external excitation is equal to zero and equilibrium at nodes L gives the following

$$[\Lambda_L]f = \{0\} \qquad where \qquad [\Lambda_L] = [I \quad 1/\lambda I] \tag{4.9}$$

In equation 4.9 note that $\{0\}$ is a vector Substituting $q = \Lambda_R q_L$ and $\Lambda_R = [I \quad \lambda I]^T$ in equation (4.1) and premultiply both sides of the equation by Λ_L, following is obtained

$$\Lambda_L[K-\omega^2 M][\Lambda_R]q_L = \Lambda_L f \quad or \quad [\lambda I \quad I]\begin{bmatrix} D_{LL} & D_{LR} \\ D_{RL} & D_{RR} \end{bmatrix}\begin{bmatrix} I \\ \lambda I \end{bmatrix} q_L = [I \quad 1/\lambda I]f \tag{4.10}$$

which can be represented in eigenvalue problem in terms of degrees of freedom of left nodes only as follow

$$[\Lambda_L K \Lambda_R - \omega^2 \Lambda_L M \Lambda_R]q_L = \{0_L\} \tag{4.11}$$

Note that zero vector $\{0\}$ is half as long as the $\{0\}$ in equation (4.9) Where

$$\bar{K} = \Lambda_L K \Lambda_R$$
$$\bar{M} = \Lambda_L M \Lambda_R$$

which are the reduced form of stiffness and mass matrices. Equation (4.11) can be further written in form of non-linear eigenvalue problem, where λ is the eigenvalue and q_L the eigenvectors denoted as follow

$$\bar{D}(\omega,\lambda)q_L = [D_{LR}\lambda^2 + (D_{LL}(\omega) + D_{RR}(\omega))\lambda + D_{RL}(\omega)]q_L = \{0_L\} \tag{4.12}$$

Here D presents the reduced dynamic stiffness matrix (DSM), which means that having n d.o.f per node, the corresponding nodal displacement and forces vectors will be $n \times 1$ and the the element mass and stiffness matrices in this case will be $2n \times 2n$, whereas the reduced matrices will be only $n \times n$. As it is seen equation (4.12) shows a relation between ω and λ, also called the dispersion relation. This equation can also be stated in generalized linear form as follows

$$\left(\begin{bmatrix} 0_{LL} & D_{LL}+D_{RR} \\ D_{LR} & D_{LL}+D_{RR} \end{bmatrix} - \lambda \begin{bmatrix} D_{LL}+D_{RR} & 0_{LL} \\ 0_{LR} & D_{LR} \end{bmatrix}\right)\left\{\begin{array}{c} q_L \\ q_R \end{array}\right\} = \left\{\begin{array}{c} 0_L \\ 0_R \end{array}\right\} \tag{4.13}$$

The null matrix 0_{LL} here has the same dimension as D_{LL}. Use of the fact that the dynamic stiffness matrix is symmetric, q_L is both a right-eigenvector associated with eigenvalue λ and a left-eigenvector related with $1/\lambda$. Therefore both λ and $1/\lambda$ are the solutions for equation (4.12), which can be written in general form as

$$\lambda = e^{(-i\gamma-\xi)} \tag{4.14}$$

(4.14) can also be written in form of complex wavenumber as follow

$$k = k_r + ik_i \qquad \gamma = k_r L \qquad and \qquad \xi = k_i L \tag{4.15}$$

In equation (4.15) γ shows the change in phase from one cell to the next one, ξ is the attenuation and L is the length of the cell[1] Chapter one. These parameters play

[1]For a better understanding of propagating, attenuating and evanescent see Figure 2.6

an important role in recognition of waves. If $\xi = 0$ or $\mid \lambda \mid= 1$ dispersion curves will demonstrate a pass-band, where energy flow will occur to the right and left of the structure. When $\xi \neq 0$ or $\mid \lambda \mid\neq 1$ no energy flow will take place and the dispersion curves will demonstrate a stop-band [Domadiya and Andersen, 2014] and [Andersen, 2015].

As demonstrated above, two types of eigenvalue problems are explained. In the first type of eigenvalue problem λ is kept unchanged and ω is determined. This type of eigenvalue problem is seen in equation (4.11). This is also the type of eigenvalue problem that is used in COMSOL, where a sweep is done over a range of wavenumbers and the corresponding eigenfrequencies are found. The other type of eigenvalue problem is the opposite of the above-mentioned eigenvalue problem. Here ω is kept unchanged and the corresponding λ values has to be determined as in equation (4.13) The above-mentioned theory will now be implemented in two examples in the following section.

4.2 Periodic one-dimensional waveguide

In this section a one-dimensional periodic waveguide will be analysed. The waveguide has two different cross sections illustrated in Figure 4.3. A unit-cell from this particular cell has the following property Table 4.1.

Table 4.1. Properties of periodic cell.

Youngs modulus E	200×10^9 Pa
Poisson's ratio μ	0,3 –
Density ρ	1000 kg/m^3
Total length of cell L	12 m

The solid model has the following geometrical properties Figure 4.3.

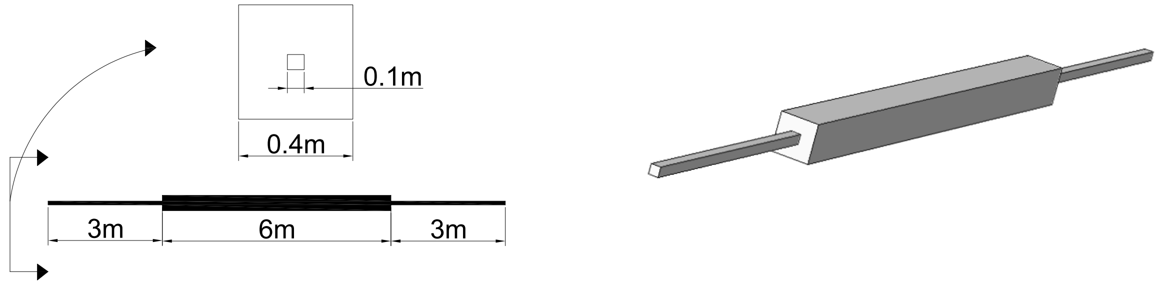

Figure 4.3. One-dimensional periodic cell build as solid model in COMSOL (right). Geometrical dimensions of one-dimensional periodic cell (left).

Where in continuous form the Figure 4.3 looks like the following Figure 4.4

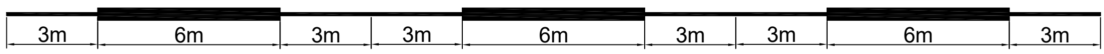

Figure 4.4. Two-dimensional illustration of the periodic structure.

4.2.1 Modelling periodic cell in COMSOL

In this section it will be shown how a periodic cell is constructed and analysed in COMSOL according to Floquet's theory. Subsequently different boundary conditions will be applied to the cell and eigenmodes from the two programmes will be extracted and compared.

1. The first step is to choose the proper physics. In this case three-dimensional model and thereafter "Solid Mechanics(solid)" is chosen and "Eigenfrequency" is chosen as the "Study". As mentioned in the previous chapter this model takes a lot of computational memory, still it was chosen as it is the only model which has the choice of periodic and Floquet's boundary condition i.e. Floquet theory cannot be applied to beam theory in COMSOL.
2. Step two is defining the parameters. It is up to ones self how many parameters one defines. In this particular case the three important parameters, **total length of the cell**, **wavenumber** and defining **wave component in x-**

direction [2]. These three parameters are unavoidable as they are recalled in further calculation.

3. The next step is building the geometry, in this case the periodic cell.
4. Thereafter assigning material to the geometry. The properties from Table 4.1 has been used.
5. Under "Solid Mechanics (solid)" periodic conditions is chosen. This boundary condition is then applied to the two ends of the cell Figure 4.3.

   Getting the frequency response, requires analysis of periodic unit cell with Block periodic boundary conditions for two-dimensional structures known as Floquet boundary conditions in one-dimensional structures. The range of wave vectors should be big enough to cover the edges of the so-called *irreducible brillouin zone* (IBZ). Following Figure 4.5 illustrated a (IBZ) for a two-dimensional rectangular structure. [Elabbasi, 2016]

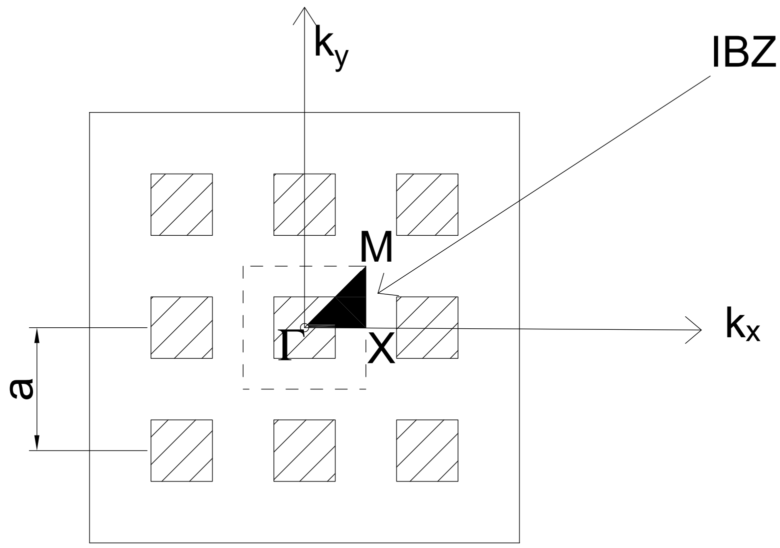

Figure 4.5. Irreducible Brillouin zone in a two-dimension periodic structure.

   As seen in the above Figure 4.5 stretches from Γ to X to M and back to Γ. The aforementioned destination and source are applied to the left and right ends of the structure.

6. The model is meshed, in this case a convergence analysis is done.
7. In "Study" section, the desired number of eigenfrequencies are chosen to be 30. Although only the first 10 eigenfrequencies which will be presented here, the reason for the high number of frequencies as mentioned in previous chapter is more double eigenfrequencies will be produced in solid model. Therefore

[2]The reason for only defining in x-direction is the waveguide is only one-dimensional periodic structure.

sufficient number of eigenfrequencies are chosen so it is easy to pick the ten eigenfrequencies out of 30.

The next step in "Study" section is adding a "Parametric Sweep". It is here the parameter **wavenumber** used in the second step comes into play. If this parameter is not defined in the second step it will not be possible to make the sweep. The idea here is to utilize the dispersion curves based on waveumber, therefore a sweep is only done on the wavenumber. The parametric sweep here ranges from 0 to 1. As mentioned previously the type of eigenvalue problem solved here is the one stated in equation (4.11). The size of the step is important, as the smaller the step is, the more time and computational memory will be consumed. This together with a very fine mesh will complicate the problem even more. The reason for choosing more steps is explains in the subsequent section.

8. Computation of the model
9. Showing results

4.2.2 Natural frequencies of the one-dimensional cell with free-free, fixed-fixed

Before applying periodic boundary conditions, first a free-free and fixed-fixed boundary conditions will be applied to the cell. This will be done in both MatLab and COMSOL. Once again this will illustrate the reliability of the results come from COMSOL, and will give a perspective on how different the COMSOL computes the results from MatLab. The model in COMSOL is built as solid. As mentioned previously there are some limitations in COMSOL. A beam model can only be build with a constant cross section, therefore building a cell with different cross sections is not possible in COMSOL (beam model). The second limitation is the lack of periodic boundary condition in beam model. So the only choice left is the solid model. Therefore in the following only solid model will be used in COMSOL. The solid model has still the same geometrical and physical properties as in Figure 4.3 and tabel 4.1.

First a convergence analysis will be done as before for finding the proper element size. The following Figure 4.6 shows the convergence analysis for COMSOL.

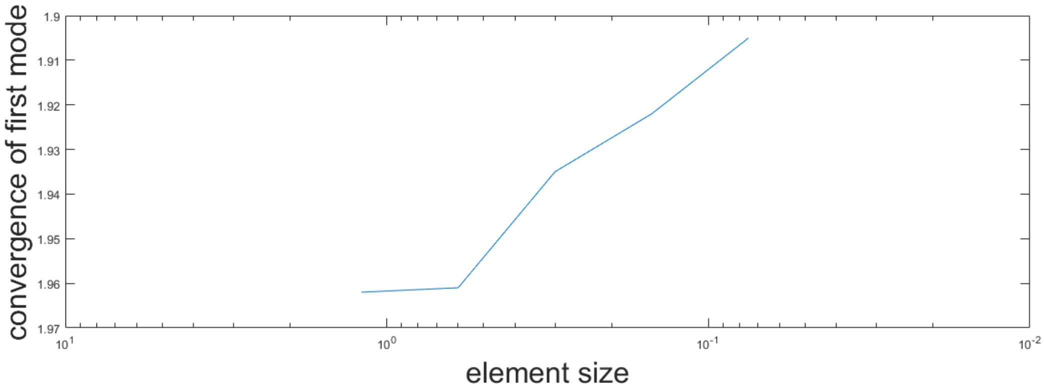

Figure 4.6. Convergence graph for unit cell build in solid model in COMSOL.

As it is seen in the Figure 4.6, the convergence is not finished yet, but based on the graph an element size of 0,075 m was found acceptable. The reason for stopping convergence was once again due to memory consumption. No convergence analysis is done for MatLab as the model was converged in a very early phase. The reason for choosing an elements size of 0,5 — was for producing sufficient eigenmodes.

Cell with a fixed-fixed boundary conditions

As done previously, the first 10 modes will be illustrated. The comparison here is done between a solid model in COMSOL and MatLab model. The first ten modes are illustrated in the following 4.7.

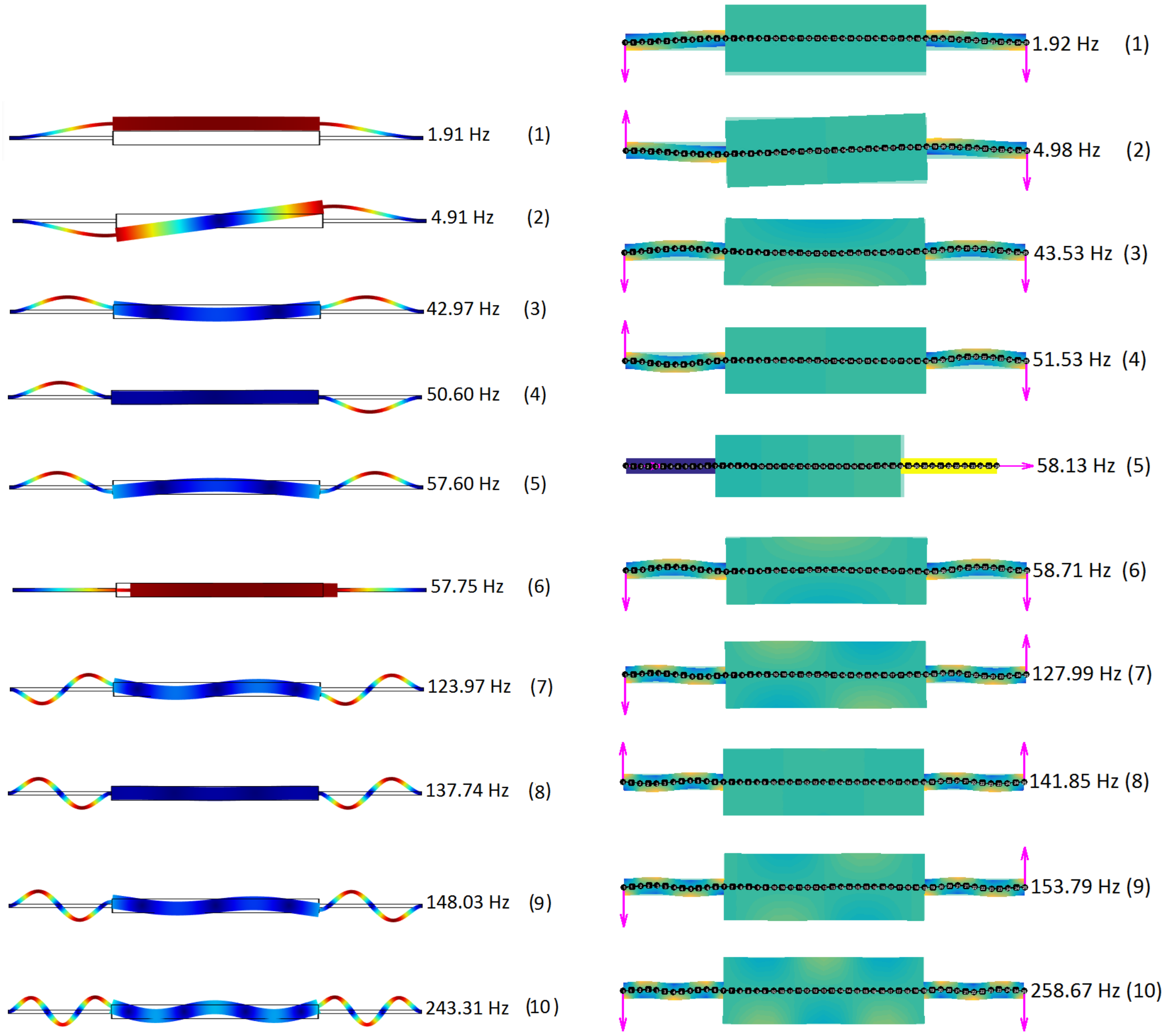

Figure 4.7. The first ten eigenmodes of a cell with fixed boundary conditions in COMSOL (left) and MatLab (right).

Once again the axial mode (mode six) appears later in COMSOL, which due to the fact that torsional modes are not illustrated here.

Cell with a free-free boundary conditions

Similarly the first ten modes of a cell with free-free boundary conditions are illustrated.

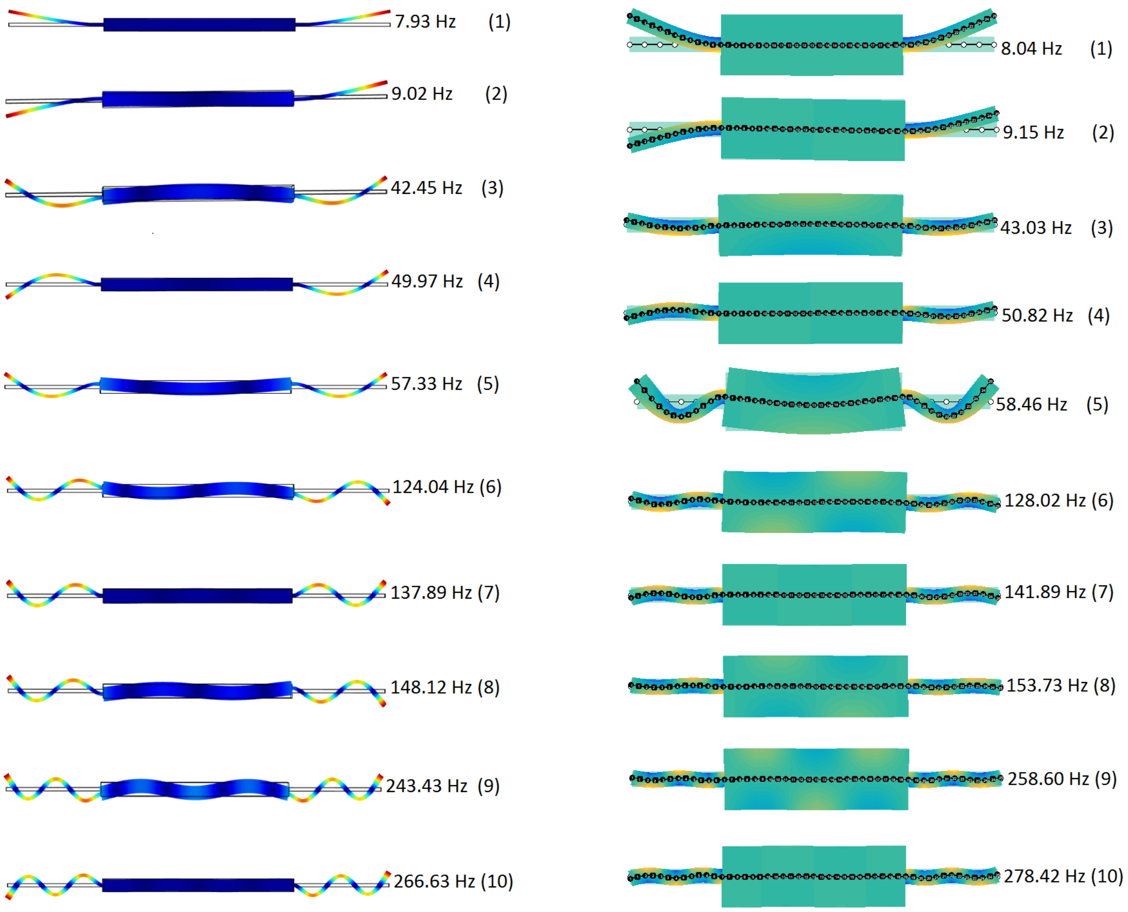

Figure 4.8. The first ten eigenmodes of a cell with free boundary conditions in COMSOL (left) and MatLab (right).

The difference between the two programs is first and foremost due to the two different models used where solid model is used in Comsol and beam model is used in matlab. This difference would have been minimal if beam model was used in both programmes. Apart from this difference both programmes give almost the same result.

As both fixed and free boundary conditions are tested in both programmes, now periodic boundary condition will be used in both programmes and demonstrated how differently COMSOL computes a cell with a periodic boundary condition from MatLab.

The above examples shows a typical impedance mismatch behaviour. In second Chapter, the impedance mismatch was related to propagation of wave from one material into another. Here the structure does not have two different materials but rather a change in the geometry. As the waves propagates from the thinner part of the cell and hits the thicker part, there will be an impedance mismatch.

Cell with a periodic boundary conditions based on Floquet's theory

In this section the same unit cell will be analysed with Floquet's boundary conditions. The analysis is done according to section 4.2.1.In both programmes the interval for wavenumber is chosen from 0.001 to 1 with a step size of 0.001 which can be illustrated in MatLab code as 0.001 : 0.001 : 1. As seen this is a large number of wavenumbers. This is not a big challenge in MatLab as the model in MatLab is built as a beam, but in COMSOL this was a very big challenge as the model build in COMSOL is solid, which consumes an enormous amount of memory. In this particular case the computer barely made it through computation with this amount of wave numbers. Having this in mind, a convergence analysis was not done, and the beam was meshed with a "normal" size mesh in COMSOL, since a fine mesh and a large number of wavenumbers will make it totally impossible to carry out this computation.

For understanding the effect of these two challenges on the results two models were built in COMSOL.

(a) A model with large number of wavenumber 0.001 : 0.001 : 1 i.e. 1000 wavenumbers and with a a "normal" elements size.
(b) A model with small number of wavenumber 0.1 : 0.1 : 1 i.e. 10 wavenumbers and a fine mesh with $0.075m$

In this section the main focus will be on model (a). Model (b) will only be used for comparison reason at the end of this section.

In the following the first 10 eigenmodes from COMSOL and MatLab are illustrated in Figure 4.9 and Figure 4.10.

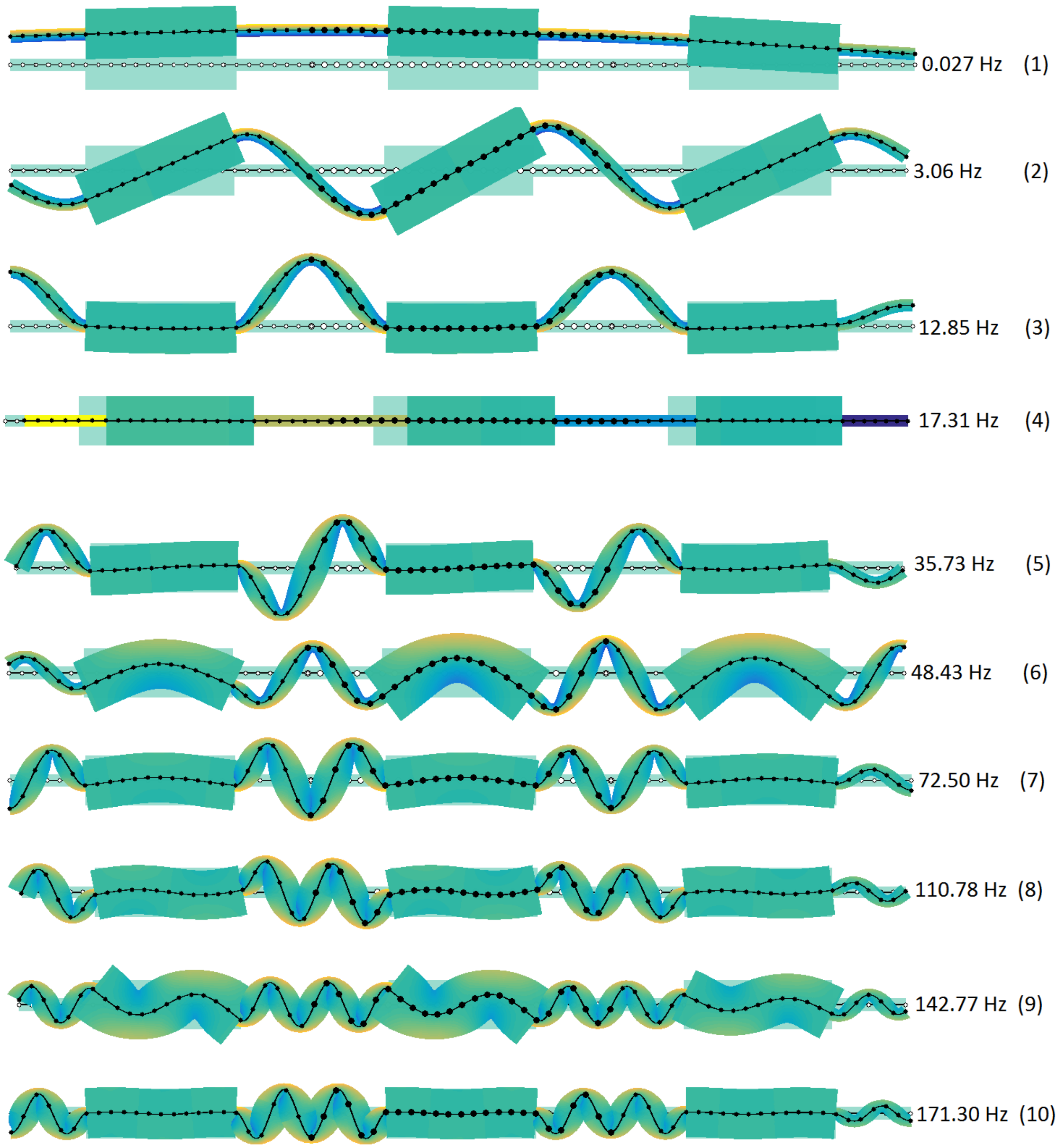

Figure 4.9. 10 MatLab modes.

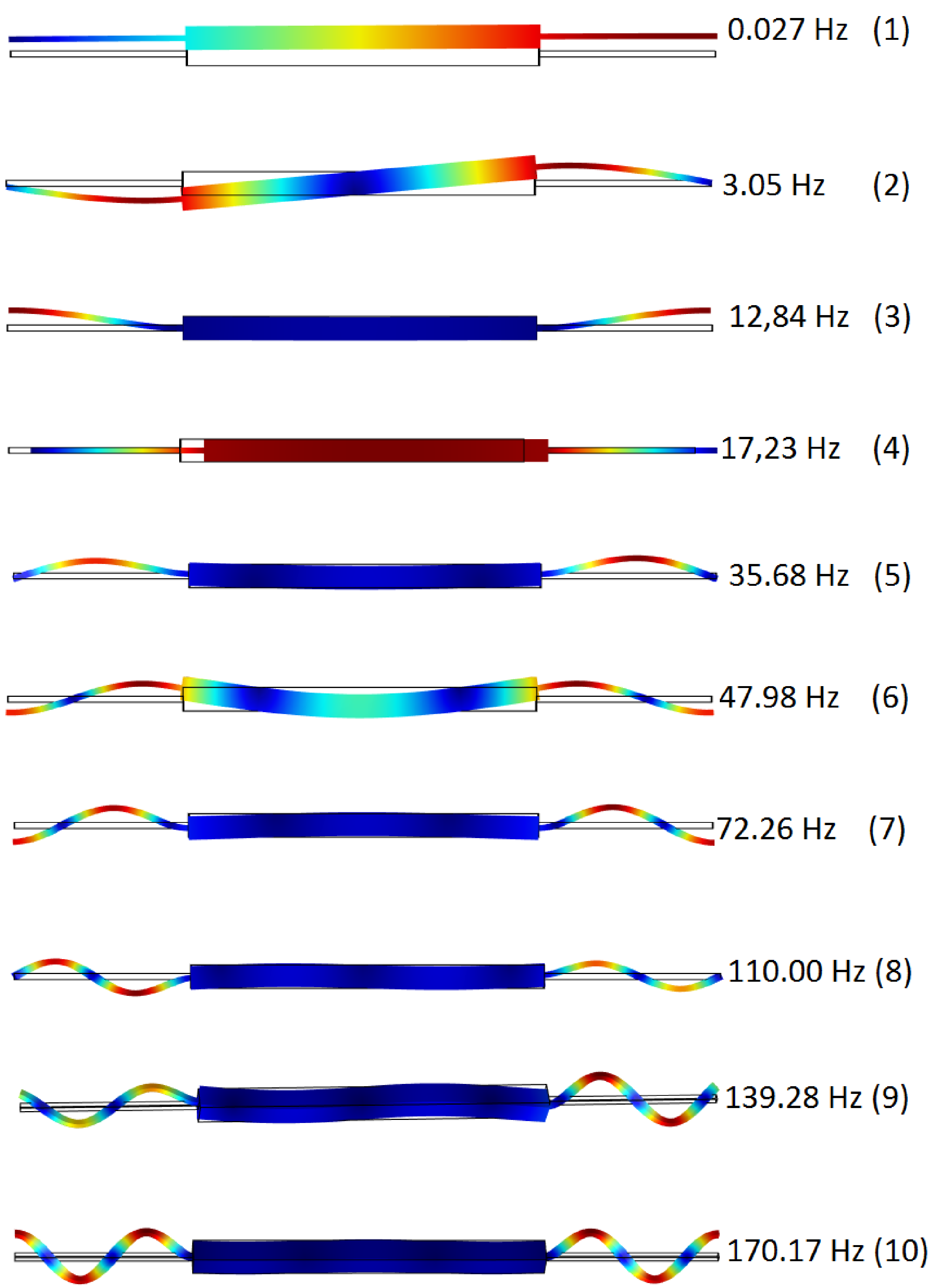

Figure 4.10. 10 Comsol modes.

The modes corresponds to a wavenumber of 0.02 in MatLab and COMSOL marked with a black horizontal line as illustrated in Figure 4.11. As it is seen in Figure 4.9 and 4.10, the modes in both programmes are really close to each other, even at higher modes the differences between the modes are not very big.

In the next step dispersion curves are plotted. As seen in the following Figures 4.11, both COMSOL and MatLab give a very similar curves, where the band gaps are clearly shown between the lines. If it is zoomed in COMSOL dispersion graph it will be noted that in many cases there are two lines representing each frequency, which is due to the double modes in a solid model. This feature cannot be seen in MatLab dispersion curves as there are only single modes.

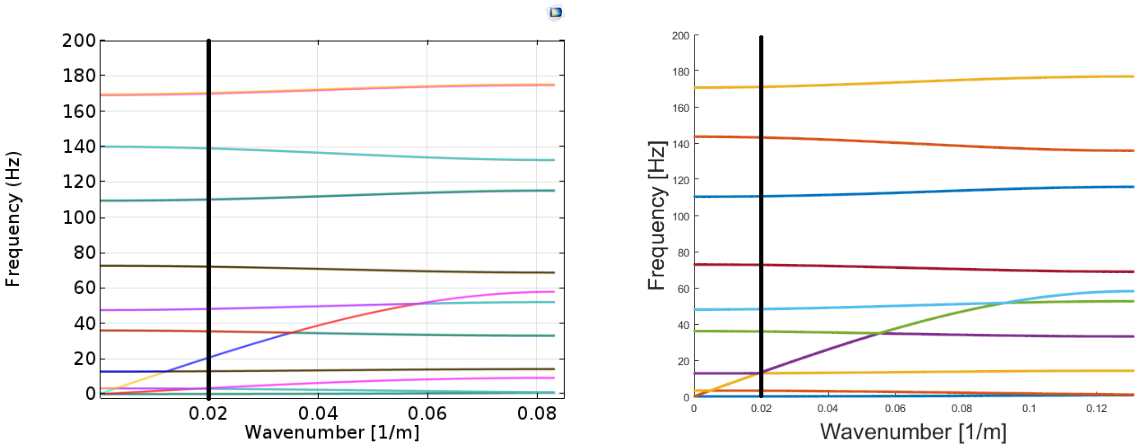

Figure 4.11. Dispersion curves for a unit cell in COMSOL (left) and MatLab (right).

The subsequent graph shows a plane plot of the wavenumbers. As seen x-axis shows the imaginary wave number in Figure 4.11 versus frequency in y-axis. The coloured line in COMSOL illustrated in Figure 4.11 on the right corresponds to the green horizontal lines and at $x = 0$ in MatLab. Once again there is a big similarity in both graphs.

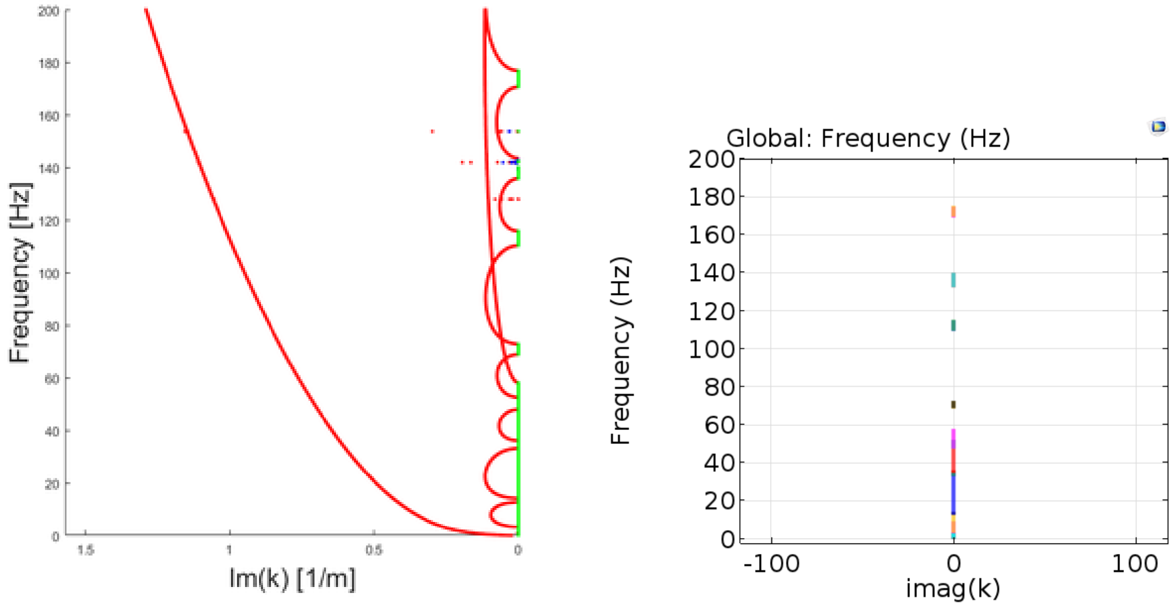

Figure 4.12. Dispersion curves for a unit cell in COMSOL (right) and MatLab (left).

Comparison of the results between models with 1000 wave numbers with normal mesh and 10 wavenumbers and fine mesh

In the following the comparison between the two aforementioned models will be done. It will be shown what influence have a large number of wavenumbers have compared to a small number and what role a fine mesh plays compared to a coarse mesh. The models from now on will be refereed to as model (a) and (b) as denoted above.

The following two areas will be compared

- The first 10 eigenmodes corresponding to a wavenumber 0.2 in both models
- Dispersion diagrams from both models

The first 10 eigenmodes are listed below

Table 4.2. Comparison tabel from left to right model (b) model (a) and MatLab.

Mode nr.	COMSOL model (b)	COMSOL model (a)	MatLab
1	0,027 Hz	0,027 Hz	0,027 Hz
1	0,027 Hz	0,027 Hz	-
2	2,656 Hz	2,824 Hz	torsional mode
3	3,025 Hz	3,050 Hz	3,06 Hz
3	3,025 Hz	3,054 Hz	-
4	12,661 Hz	12,814 Hz	12,85 Hz
4	12,663 Hz	12,837 Hz	-
5	17,191 Hz	17,233 Hz	17,31 Hz
6	35,123 Hz	35,600 Hz	35,73 Hz
6	35,128 Hz	35,677 Hz	-
7	47,777 Hz	47,974 Hz	48,43 Hz
7	47,777 Hz	47,974 Hz	-
8	70,930 Hz	72,072 Hz	72,50 Hz
8	70,940 Hz	72,257 Hz	-
9	107,970 Hz	109,840 Hz	-
9	107,990 Hz	110,00 Hz	110,78 Hz
10	137,200 Hz	139,270 Hz	-
10	137,200 Hz	139,280 Hz	142,77 Hz

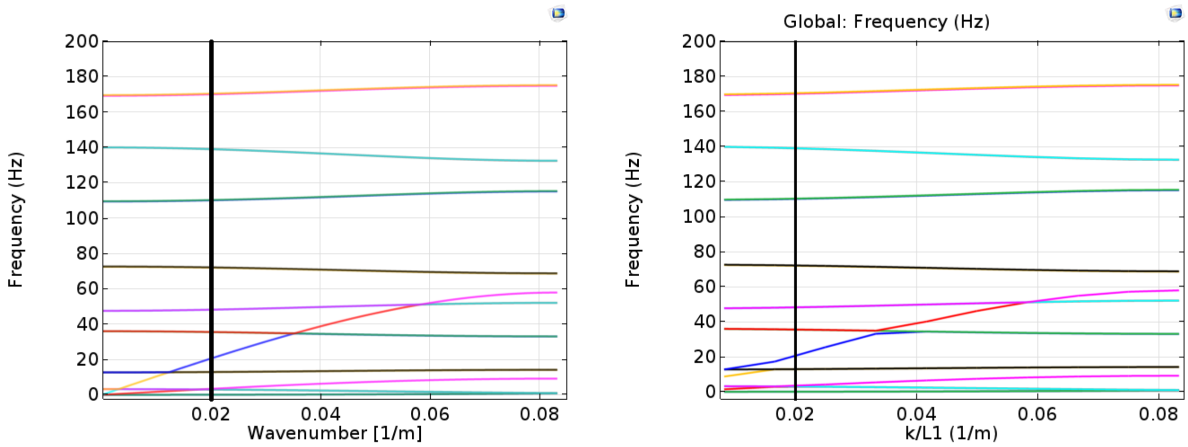

Figure 4.13. Dispersion curves for a unit cell in COMSOL. In Figure to the right 10 wavenumbers are used, where 1000 wavenumbers are used to the Figure to the left.

Dispersion diagrams in Figure 4.13 clearly shows the effect of a large number of wavenumbers compared to small number. In case a large number of wavenumbers are used the dispersion curves are very smooth and continuous whereas using small number of wavenumber, the dispersion curves are not very smooth which is obvious as there is not enough data to plot a smooth curve, for example the interval from $x = 0.2$ to $x = 0.4$ crossing $y = 17$ til $y = 38$. For the wavenumber corresponding to 0.2 the effect of the mesh can also be clearly observed as the model with fine mesh gives somewhat smaller values compared to the model with normal mesh in table 4.2. All the MatLab and COMSOL files are located in the appendix CD under the folder of "periodic cell with periodicity in one dimension".

4.3 Periodic analysis of a complex geometry based on Floquet's theory

In the previous section a periodic cell with Floquet't boundary condition was analysed where the periodicity was only in one dimension.

As shown above COMSOL delivers very reliable results, therefore a simultaneous MatLab analysis is not found necessary in this section. As from now on the results presented will only be in COMSOL.

Contrary to the previous section this section will deal with a cell, where the periodicity is in two dimension. The cell in the previous section was made of two different cross sections, which was the main characteristic of the cell. The geometric characteristics of the cell in this section are different, which will be explained in details in the following.

The cell in this section is quadratic frame of $1\,\mathrm{m} \times 1\,\mathrm{m}$ with a plate of same dimension on top of it as in Figure 4.14. The plate has the thickness of $0.015m$

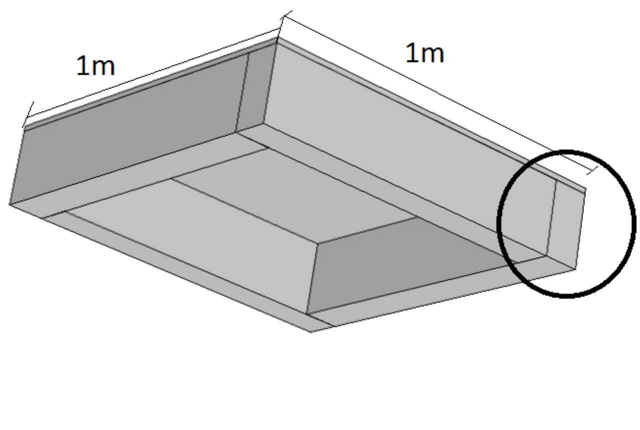

Figure 4.14. Picture of the cell taken from the bottom.

The cross section circled in the Figure will have different sizes. The cell has the following physical properties listed in table 4.3.

Table 4.3. Properties of periodic cell.

Youngs modulus E	11×10^9 Pa
Poisson's ratio μ	0.369−
Density ρ	$900\,\mathrm{kg/m^3}$
Total length of cell L	1 m

In the previous section the geometry of the cell was kept constant, and the focus was more on study of periodicity in one-dimensional waveguide. In this section apart from periodicity in two dimensions, the geometry of the cell will be varied and the corresponding dispersion curves will be studied as the geometry is varied. The dispersion curves from different sizes will then be compared.

This section is built of two parts.

In the **first** section four different sizes of cross sections will be studied. These cross sections are illustrated below. These four different sizes are referred to the area circled in Figure 4.14 i.e. the cross section of the four beams that builds the frame of the cell.

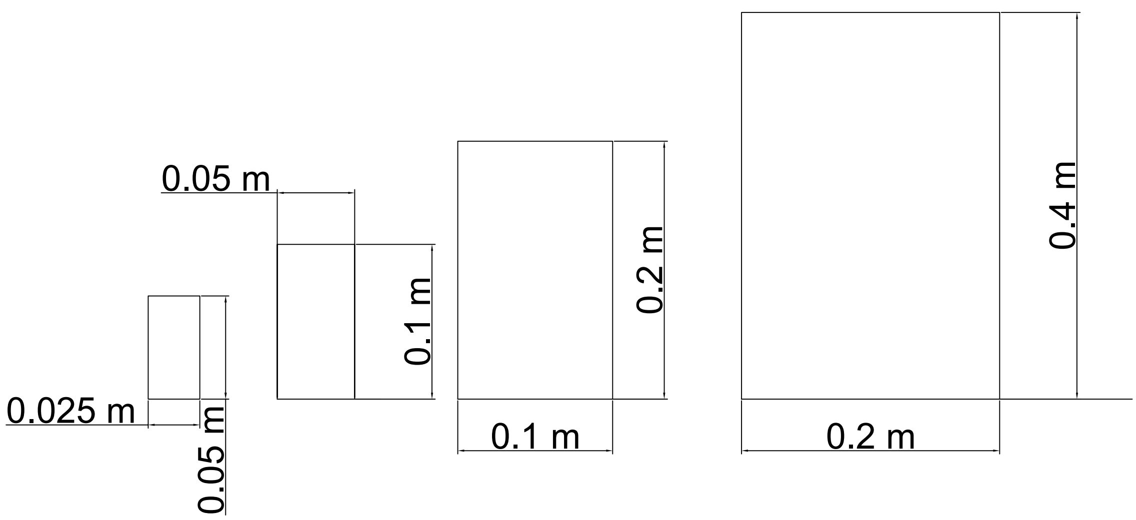

Figure 4.15. Four different sizes of cross sections used in analysis of the cell.

The following Figure shows these sizes in three dimensions

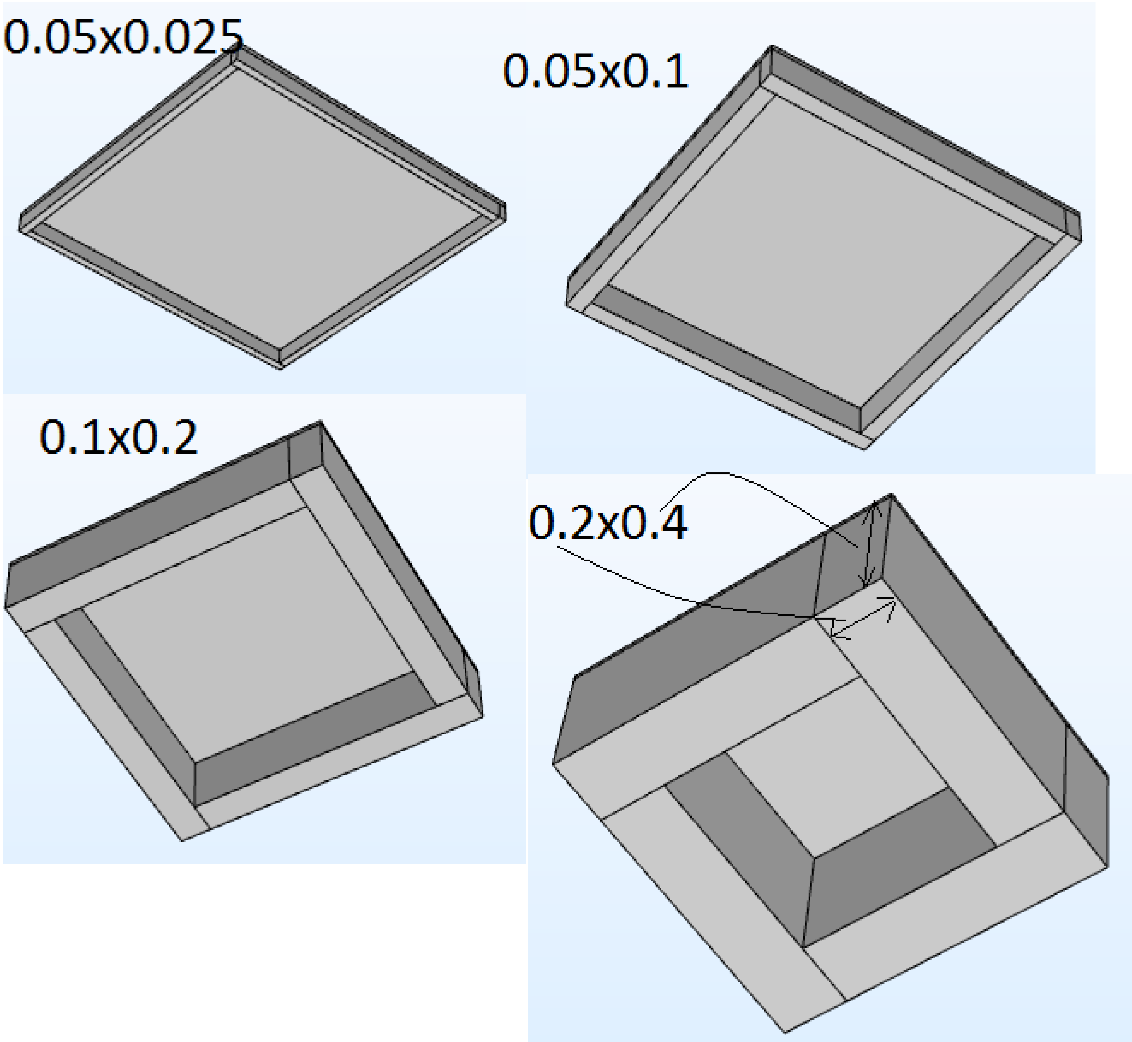

Figure 4.16. Four different sizes of cross sections in three-dimension used in analysis of the cell.

In Figures 4.16 above as seen the cell is still a $1\,\mathrm{m}\times1\,\mathrm{m}$ quadratic cell, the only change is in the cross section of the beams which builds the frame. The lengths of the beams and the dimensions of the top plate are kept constant.

Once again the first 10 modes and the dispersion curves will be compared from the above four cells and illustrated. First the dispersion curves will be illustrated for the above four Figures in Figure 4.17 and 4.18

The dispersion curves for the above four different sizes are plotted in Figure 4.16. It shall be mentioned that the original dispersion curves can be seen in appendix A.1 and A.2 . Here the y-axis is only plotted up to 1300 Hz, for comparison purpose, so the difference between the dispersion curves from these different sizes can be observed.

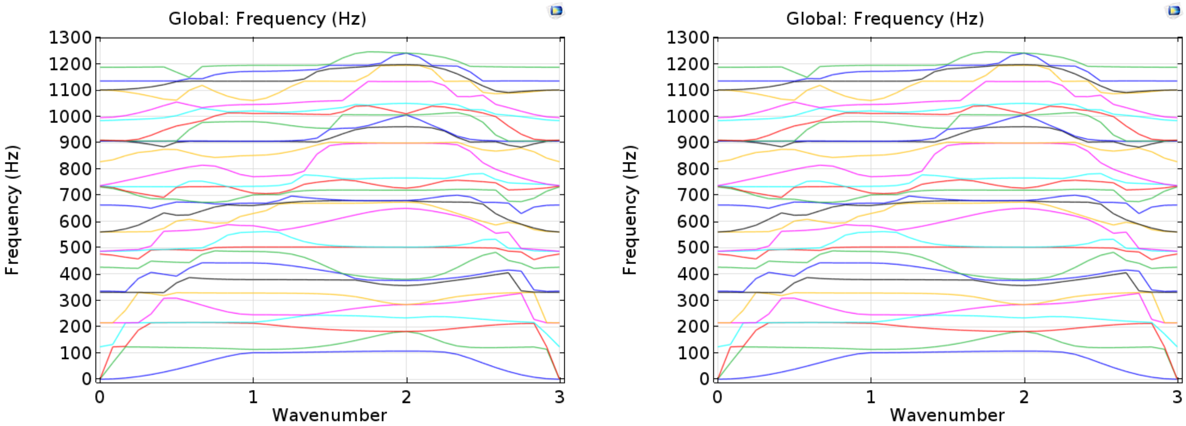

Figure 4.17. Dispersion curves for a unit cell with beam of cross section 0,025 m×0,05 m left and 0,05 m×0,1 m right.

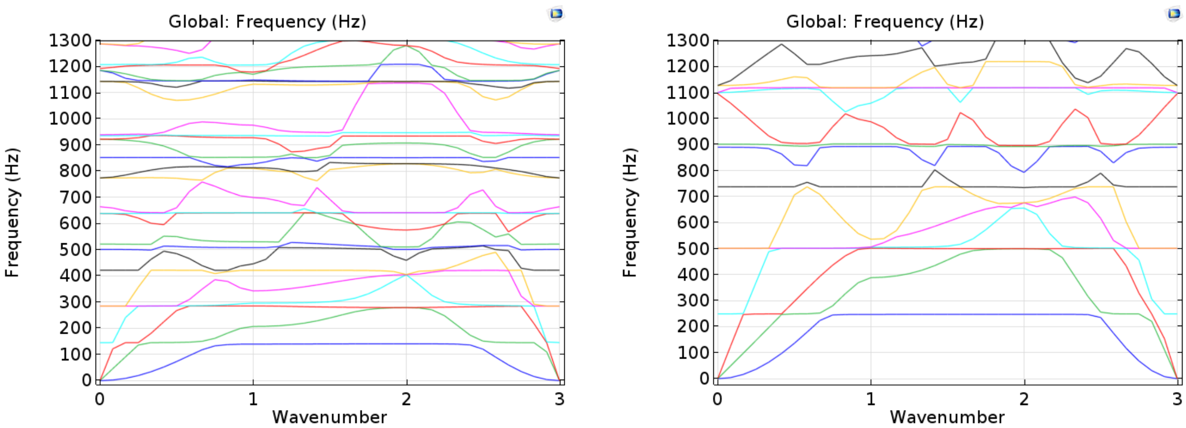

Figure 4.18. Dispersion curves for a unit cell with beam of cross section 0,1 m×0,2 m left and 0,2 m×0,4 m right.

As the dimensions of the beams in frame get bigger the frequencies appears higher in y-axis. No apparent band gaps are seen in the dispersion diagrams.

The first 10 eigenmodes are shown bellow.

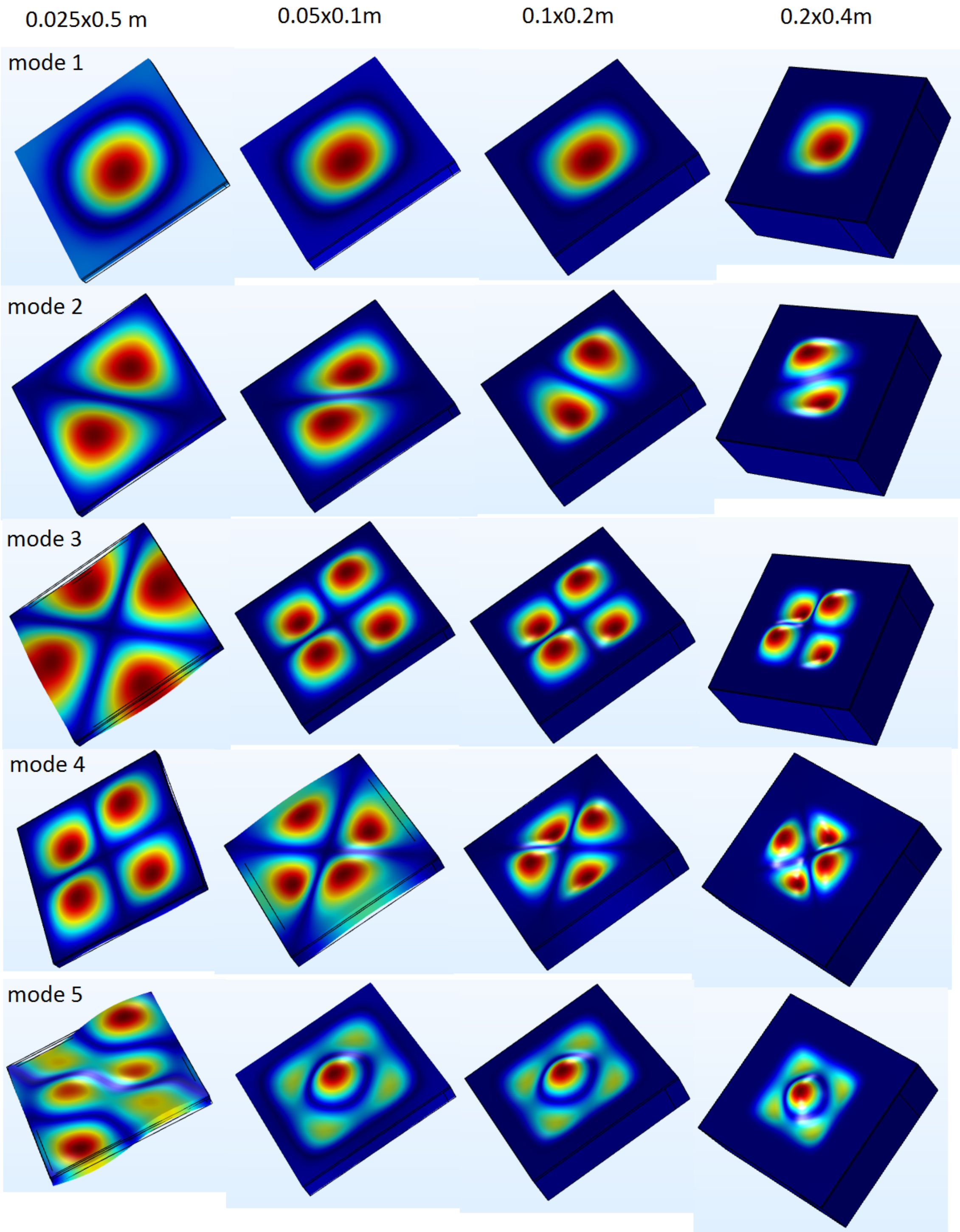

Figure 4.19. Mode one to five for all four sizes.

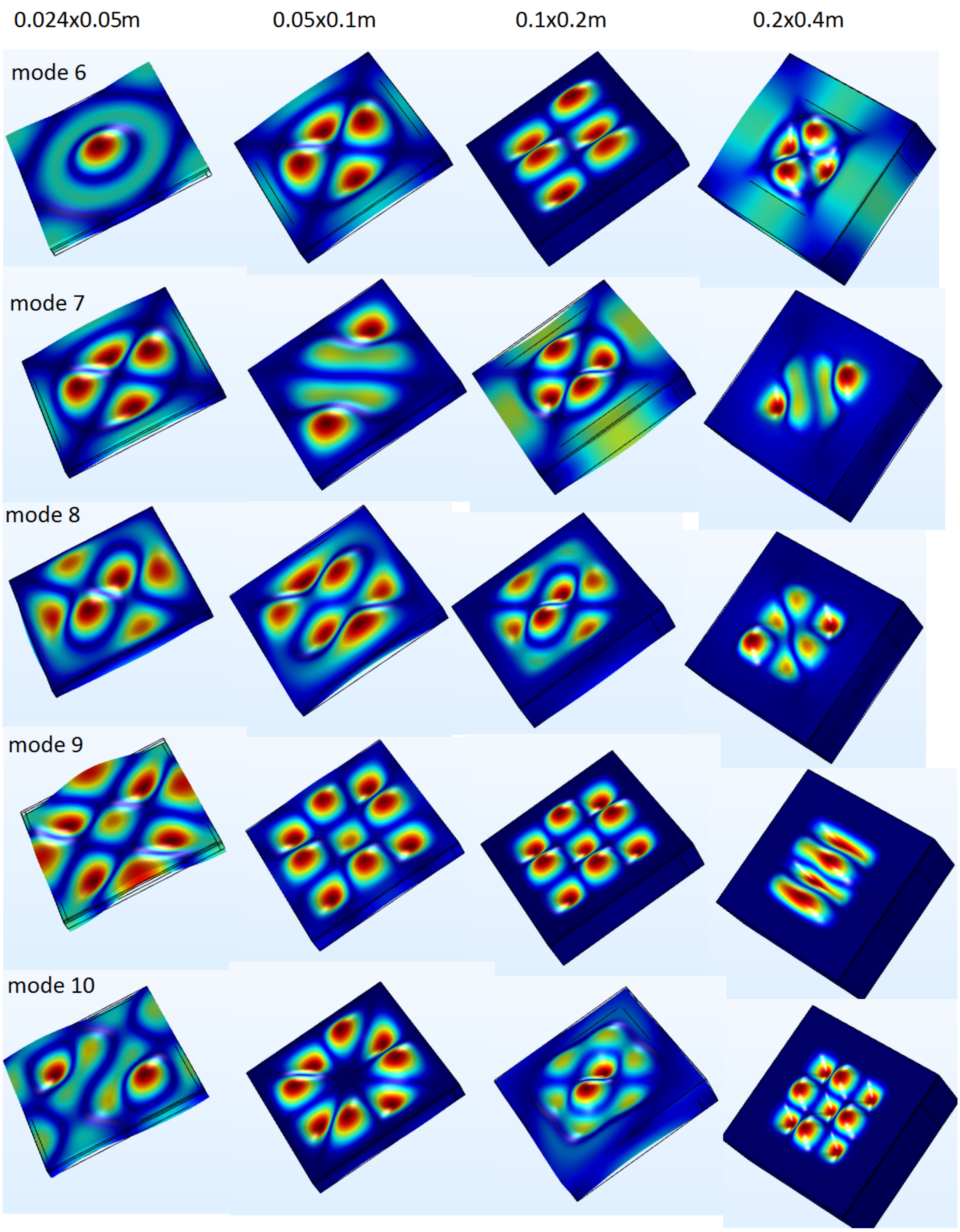

Figure 4.20. Mode six to ten for all four sizes.

All the modes above are plotted with a wavenumber of $k = 0$. Taking a look at Figure 4.19 and 4.20, it is clear that the frame in the geometry of $0.025m \times 0.05m$ has a very small or no influence on the cell. The whole cell acts like a plate rather than a plate attached to a frame. Here the frame gets deformed already in second mode. The influence of the frame gets bigger as the cross section of the frame gets thicker. This can already be seen in the next geometry of $0.05m \times 0.1m$. The first four modes in this geometry behave similar to the thicker ones like in $0.1m\times0.2m$ and $0.2m\times$ $0.4m$. The last two geometries of $0.1m\times$ $0.2m$ and $0.2m\times$ $0.4m$ deliver almost the same modes, where the frame does not get involved in deformation until higher modes as the frame is much stiffer due to its thickness compared to the plate on top. The plate here behaves like a thin sheet compared to the thick frame and the frame first gets involved in deformation in higher frequencies.

The **second** part deals with almost the same problem. Contrary to the first part where both dimensions in the cross sections (the height and the width) were varied, here the variation will only happen in one dimension namely the height of the cross section, the area circled in Figure 4.14. This variation is better illustrated in the following Figure 4.21, where all the dimensions of the cell are kept constant apart from the above-mentioned height.

Again four different sizes are chosen, shown in the following.

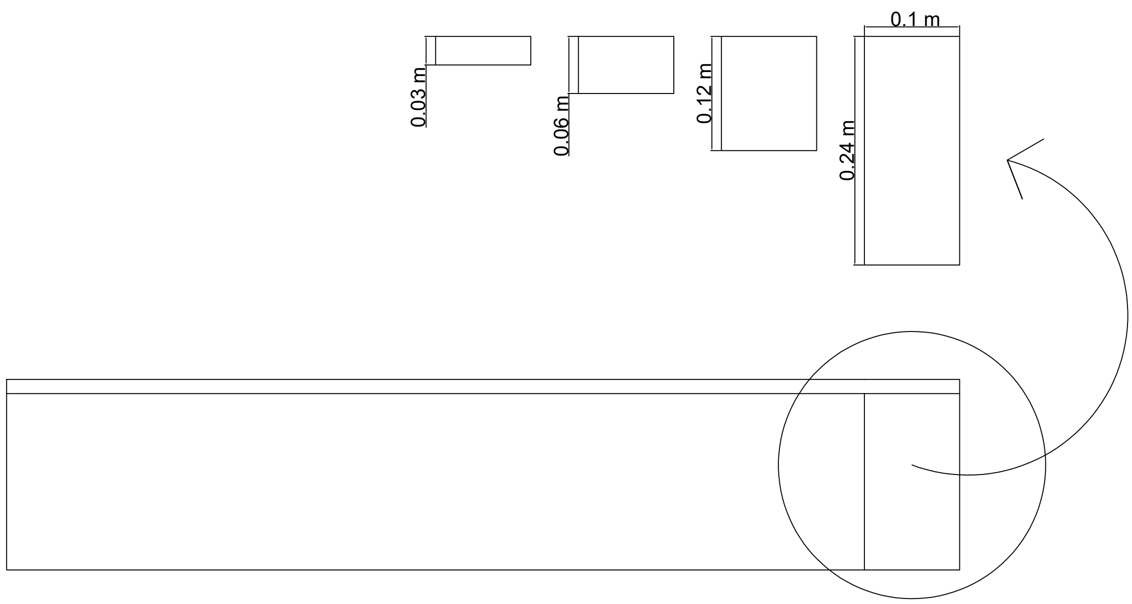

Figure 4.21. Four different sizes of cross sections used in analysis of the cell. The width is kept constant and the height varies.

Once more the dispersion curves will be illustrated and commented.

After analysis the dispersion curves are plotted below.

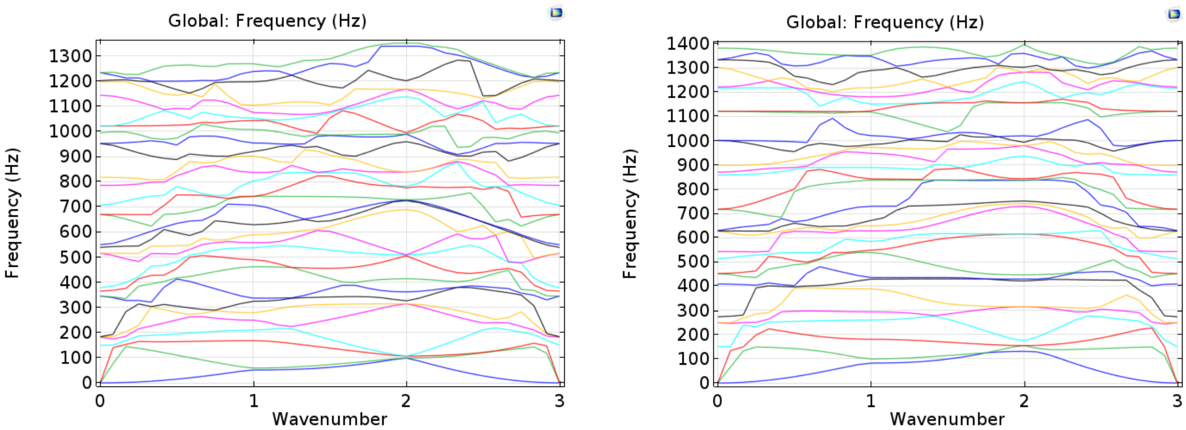

Figure 4.22. Dispersion curves for a unit cell with the cross section of 0,1 m×0,03 m left and 0,1 m×0,06 m right.

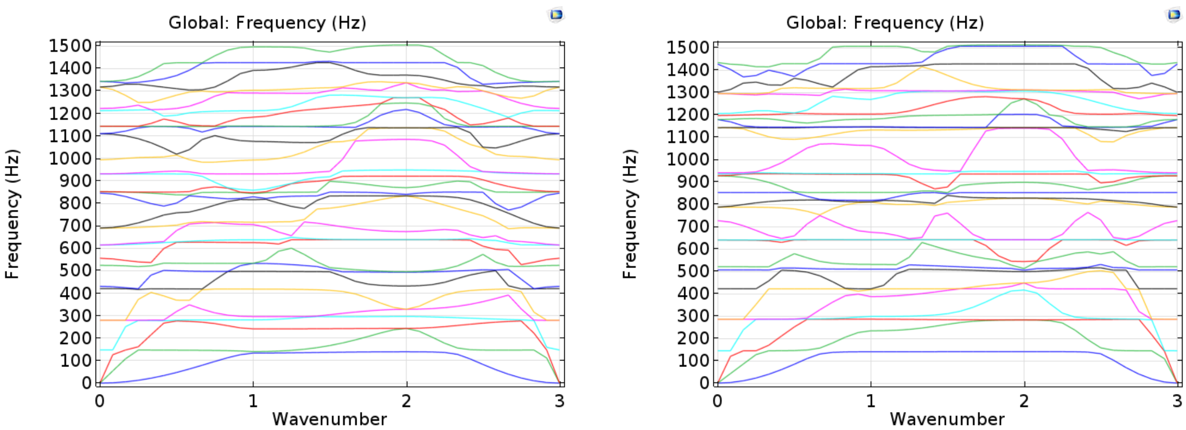

Figure 4.23. Dispersion curves for a unit cell with cross section of 0,1 m×0,12 m left and 0,1 m×0,24 m right.

Once again no band gap appears in any of the dispersion diagrams. Observing the frequency around 100 Hz (the first blue line from the bottom), the diagrams in 4.22 are similar to each other the accordingly the diagrams at 4.23 are similar to each other.

The eigenmodes for these models are chosen not to be plotted here as they were more similar to the modes plotted in Figure 4.19 and 4.20.

4.4 Additional models

Due to curiosity, some extra models were built for a better understanding of dispersion curves. The following two models are analysed.

1. **Model 1** Instead of two-dimension the cell is only given one-dimensional periodic boundary conditions.
2. **Model 2** The top plate is changed to a steel plate, where the frame has still the same material as previous. The cell will still have periodicity in two-dimensions.

Model 1

In the first model, one of the cells which has the dimensions of 0,2 m×0,4 m is given periodic boundary conditions only in one direction as mentioned above. The dispersion curves are plotted in the following Figure 4.24

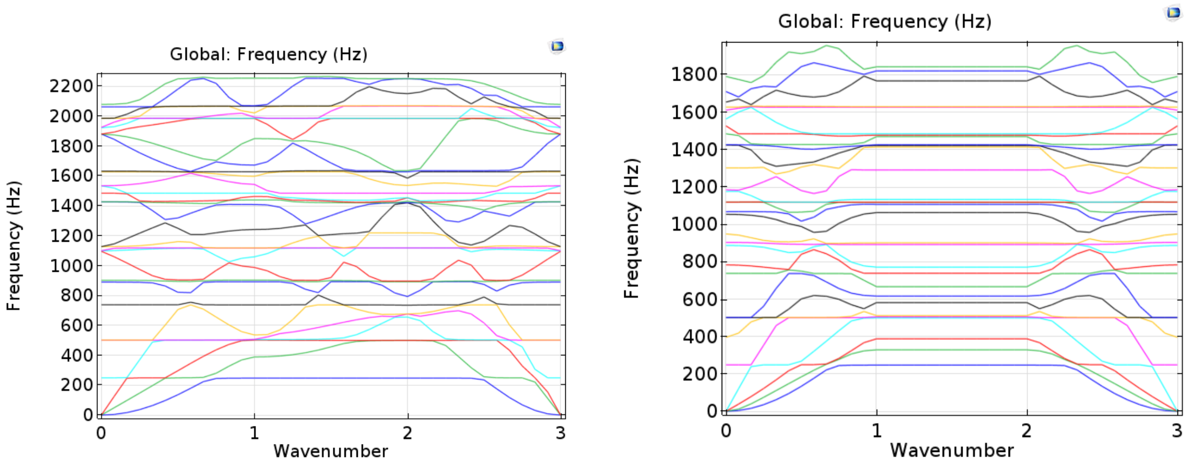

Figure 4.24. Dispersion curves for a unit cell with periodic boundary conditions in two-dimensions left and dispersion curves for a unit cell with periodic boundary conditions in one-dimensions right.

Interestingly the major difference in both curves in the above diagrams is on the x-axis where in the interval between 1 and 2 the curves for one-dimension periodicity gives straight lines. This interval corresponds to the interval between the space between X and M in Figure 4.5 on page 49. As there is no periodicity y-direction and this X-M interval is in y-direction, therefore the dispersion curves deliver straight lines in this interval.

Model 2

In this particular case the top plate was switched with a steel plate. Here all the dimensions are kept constant but the structure is made of two different types of material, where the frame of the structure is the same material as before and the top plate of the structure is made of steel.

It is assumed that since the steel plate has a higher stiffness compared to the existing material, therefore the dispersion curves will be similar to the ones where the frame was thin compared to the plate as in Figure 4.17 to the left and 4.22 to the left, where the frame had a very little effect in the modes. It is also assumed that the modes will be somewhat similar to the aforementioned Figures.

The dispersion diagrams are plotted in the following.

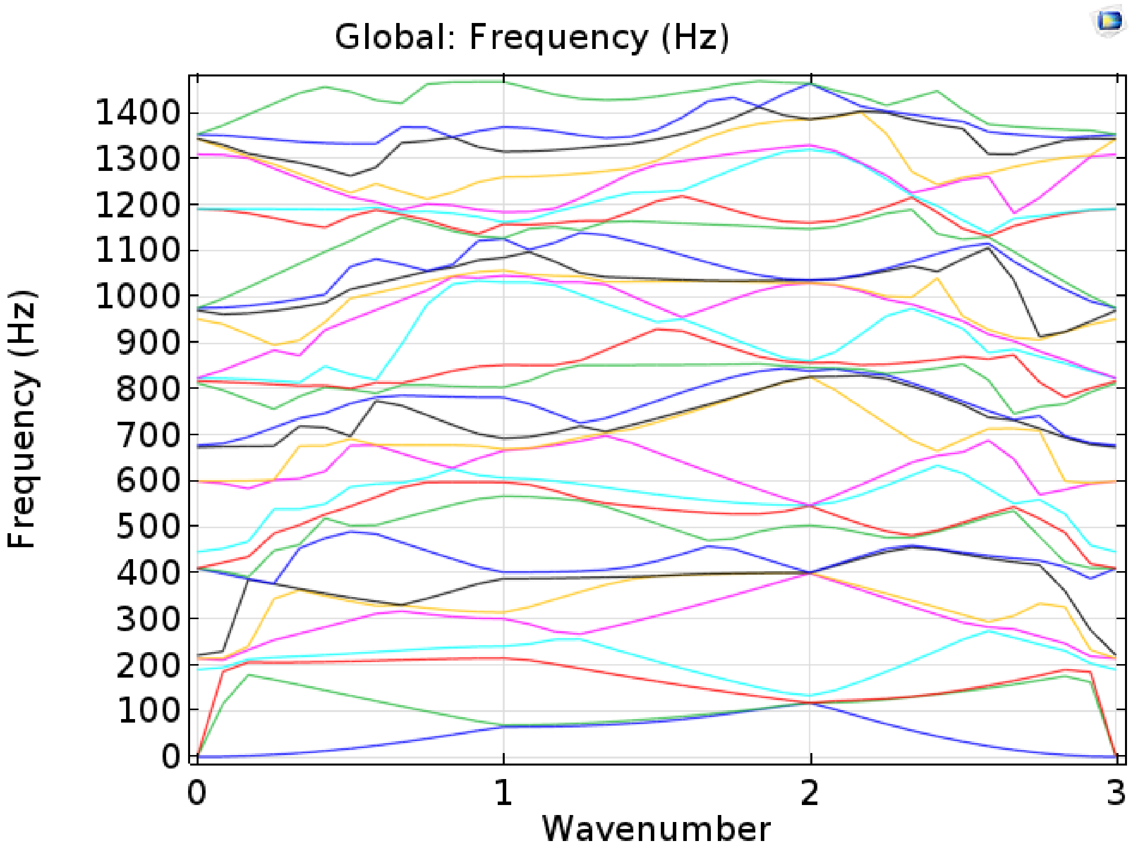

Figure 4.25. Dispersion curves for a periodic cell with a steel top plate.

As assumed the dispersion diagram in Figure 4.25 is closer to the ones that have a thinner frame rather than thicker frame, which makes sense. Once again observing the frequencies around 100 Hz (the blue line at the bottom of the Figure 4.25), it is seen that the curves have similarity to the one in Figure 4.22 on the left with the cross section of 0,1 m×0,03 m.

All the models for COMSOL are located in the appendix CD under folder of "Periodic cell with periodicity in two-dimensions"

5 Conclusion and discussion

The project starts by an introduction to vibration and explains how the waves propagate through elastic media. Furthermore reflection and transmission are illustrated and explained. As these subjects were clarified, a solution has to be chosen to deal with the challenge of vibration. In this case among many solutions periodicity in structure and civil engineering was chosen as the solution for attenuation of vibration. In first part of the project the work of some scientists in this area is presented. Through their articles it was illustrated that different types of periodic structures can be used in different areas of civil and structural engineering. Moreover their effect in regard to attenuation of vibration was shown, which proved to be very effective. Dispersion curves are a very common term in most of these articles, where the authors have tried to illustrate the bang gaps with the help of plotting these curves. Another common method frequently used in most of these articles is Floquet's theory, where most scientists have expressed their satisfaction by using this theory, since this theory makes the problem of periodicity much more simple.

Modelling and dynamic analysis of periodic structures is considered a complicated subject in this project, therefore chapter two starts with a simple approach, by explaining the basics of finite elements theory in dynamics. In this chapter the reader gets familiar with the concept of dynamic analysis of a simple structure for example a beam before moving on to dynamic analysis of a periodic structure. As the subject of natural frequencies of a beam with fixed-fixed and free-free boundary conditions are described, one-dimensional periodic boundary conditions based on Floquet's theory are presented for a unit cell. This is done in commercial software COMSOL multiphysics and MatLab and the results were compared. It was shown that COMSOL results were in accordance to MatLab. This approval by MatLab was important before moving on. Accordingly the dispersion curves were plotted and compared, they proved to be very similar to each other. The comparison of these curves was not quite simple as it was not known to which extent the model in COMSOL was fully converged. This problem was due to insufficient computational memory. Despite of all these challenges COMSOL delivered very reliable results which were in a very good accordance to MatLab.

As in this stage of project the reader gets more familiar with the concept of periodicity, a somewhat complicated cell was built. The cell was given periodic boundary conditions in two directions. In this phase the approval from MatLab program was not found necessary, the focus instead was more on observing the dispersion diagrams and optimization of the geometry. Two models with four different inner sizes. Each were analysed and their dispersion diagrams were compared to each other. As expected the dispersion diagrams were different for each of these geometries. There were some similarities between some of the curves, which was due to the somewhat closer sizes. Accordingly their modes were plotted. The transition between the sizes from the smaller frame to the biggest frame was clearly visible. The modes also demonstrated the influence of the thickness of the frame in the cell.

Plotting dispersion relation between the wavenumber and frequencies was interesting, therefore two other models were also analysed. In the first model the cell was built of two different materials and the second model the cell was given periodic boundary conditions only in one-dimension, so the curves could be compared with the same cell of having periodic boundary conditions in two-dimensions. From these two models the last mentioned model gave more interesting dispersion curves among the two, where nothing surprising was observed in the second model where the cell was made of two different materials.

It can be concluded that COMSOL is considered the ideal software for this project. Through the whole project the software gave a very few challenges in modelling periodic structures. There are also many other options available in the programme such as plotting options. Here the user has the option of plotting a variety of diagrams and relations between different parameters. Another options is the so-called parametric sweep. As described through the project, parametric sweep gives the user the option to choose a number of values or an interval with definite steps for a certain parameter, The programme will then compute the parameter according to each of those values or steps, which in this case it was done for wave numbers. This parametric sweep can be done for any defined parameter.

There is also a downside to the programme, which was also the challenge in this project. This challenge which is also mentioned through the project was the limitation of periodic boundary condition in beam models in COMSOL. Availability of this option in beam models will save a lot of computational memory and time.

Bibliography

Andersen, 2006. Lars Andersen. *Linear Elastodynamic Analysis*. ISSN: 1901-7286. Aalborg University Deparment of Civil Engineering DCE Lecture Notes No.3, 2006.

Andersen, 2015. Lars Vabbersgaard Andersen. *Using periodicity to mitigate ground vibration*. COMPDYN 2015 5th ECCOMAS Thematic Conference on Computational Methods in Structural Dynamics and Earthquakse Engineering, 2015.

Andersen and Nielsen, 2005. Lars Vabbersgaard Andersen and S.R.K. Nielsen. *Reduction of ground vibration by means of barriers or soil improvement along a railway track*. Soil Dynamics and Earthquake Engineering 25 (2005 701-716), 2005.

A.Y.-T.Leung, 1980. A.Y.-T.Leung. *Dynamic analysis of periodic structures*. Journal of Sound and Vibration (1980(4), 451-467, 1980.

Domadiya and Andersen, 2014. Marcello Vanali Andrea Ricci Domadiya, Elisabetta Manconi and Lars V Andersen. *Numerical and experimental investigation of stop-bands in finite and infinite periodic one-dimensional structures*. DOI: 10.1177/1077546314537863. Journal of Vibration and Control (2016), Vol. 22(4) 920-931, 2014.

Elabbasi, 2016. Nagi Elabbasi. *Modeling phononic band gap materials and structures*. COMSOL BLOG, 2016. URL `https://www.comsol.com/blogs/modeling-phononic-band-gap-materials-and-structures/`.

Gaofeng and Zhifei, 2010. Jia Gaofeng and Shi Zhifei. *A new seismic isolation system and its feasibility study*. Earthq Eng and Eng Vib (2010) DOI: 10.1007/s11803-010-8159-8. School of Civil Engineering, Beijing Jiaotong University Beijing 100044, China, 2010.

H J Xiang and Mo, 2012. S J Wang H J Xiang, Z F Shi and Y L Mo. *Periodic materials-based vibration attenuation in layered foundation: experimental validation*. IOP Science, 2012.

Huang and Shi, 2013. Jiankun Huang and Zhifei Shi. *Application of Periodic Theory to Rows of Piles for Horizontal Vibration Attenuation.* American Society of Civil Engineers, 2013.

Jeong and Ruzzene, 2004. Sang Min Jeong and Massimo Ruzzene. *Directional and band-gap behavior of periodic grid-like structures.* Smart Structures and Materials 2004: Damping and Isolation, DOI:10.1117/12.540352, Vol.5386. School of Aerospace Engineering, Georgia Institute of Technology, Atlanta GA, 30332, 2004.

Jeong and Ruzzene, 2005. Sang Min Jeong and Massimo Ruzzene. *Experimental analysis of wave propagation in periodic grid-like structures.* Smart Structures and Materials 2004: Damping and Isolation, DOI:10.1117/12.599709. School of Aerospace Engineering, Georgia Institute of Technology, Atlanta GA, 30332, 2005.

L.Hinke and Brennan, 2004. B.R. Mace L.Hinke and M.J. Brennan. *Finite element analysis of waveguides.* ISVR Technical Memorandum No 932. University of Southampton, 2004.

Mead, 1974a. D.J. Mead. *Wave propagation and Natural modes in periodic systems: I mono-coupled systems.* Journal of sound and vibration (1975) 40(1); 1-18, 1974.

Mead, 1974b. D.J. Mead. *Wave propagation and Natural modes in periodic systems: II Multi-coupled systems, with and without damping.* Journal of sound and vibration (1975) 40(1); 19-39, 1974.

Mead, 1969. D.J. Mead. *Free wave propagation in periodically supported infinite beams.* Journal of sound and vibration (1970) 11(2); 181-197, 1969.

M.Ruzzene and Scarpa, 2003. M.Ruzzene and F Scarpa. *Ageneral FEM technique to model wave propagation in cellular periodic structures.* Smart Structures and Materials 2003: Behaviour and Mechanics, DOI:10.1117/12.599709. School of Aerospace Engineering, Georgia Institute of Technology, Atlanta GA, 30332, 2003.

Q. Gao and Williams, 2012. F. Wu H. W. Zhang J. H. Lin W. P. Howson Q. Gao, W. A. Yao and F. W. Williams. *An efficient algorithm for computing the dynamic respones of one-dimesional periodic structures and periodic structures with defects.* DOI: 10.1007/s00466-012-0829-0. Springer-Verlag Berlin Heidelberg 2012, 2012.

R.D. Cook, 1989. M.E. Plesha R.D. Cook, D.S Malkus. *Concepts and applications of finite element analysis*. Fourth edition. John Wiley and Sons, 1989.

Takemiya and Shimabuku, 2002. Hirokazu Takemiya and Jorge Shimabuku. *Application of soil-cement columns for better seismic design of bridge piles and mitigation of nearby ground vibratio due to traffic*. Journal of structural engineering Vol.48A(March 2002), 2002.

Bilag A

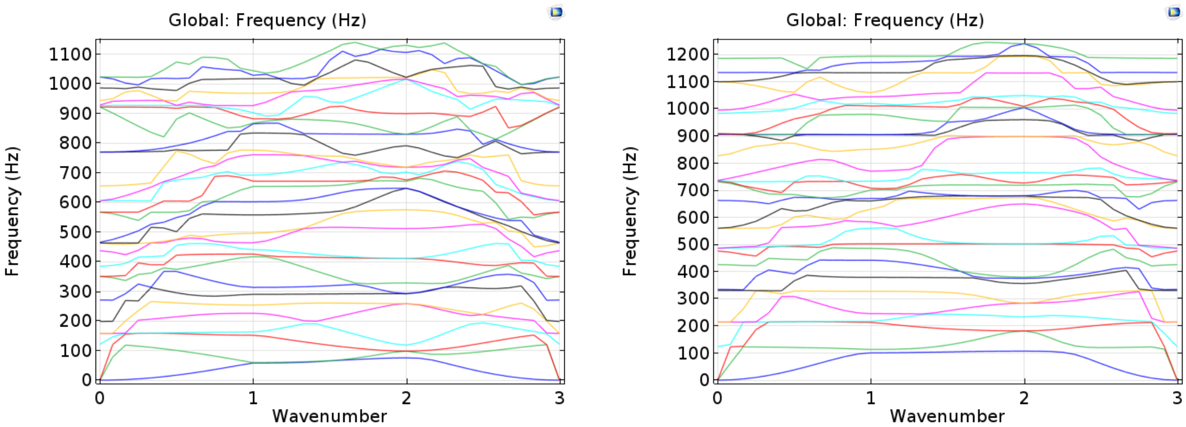

Figure A.1. Dispersion curves for a unit cell of 0,025 m×0,05 m left and 0,05 m×0,1 m right.

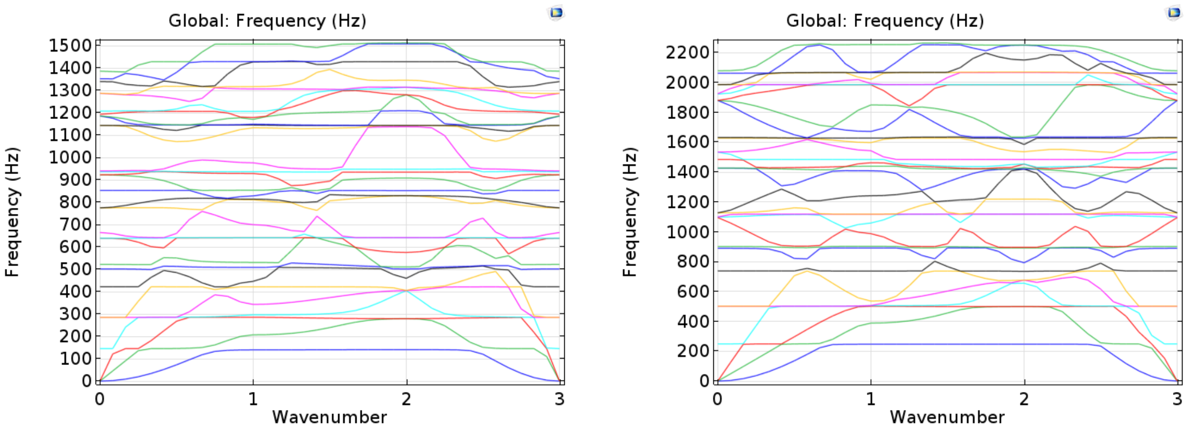

Figure A.2. Dispersion curves for a unit cell of 0,1 m×0,2 m left and 0,2 m×0,4 m right.